From CO_2 to formic acid fuel cells

*Zhenni Ma[a], Ulrich Legrand[a], Ergys Pahija[a], Jason R. Tavares[a], Daria C. Boffito[ab,]**

[a] Department of Chemical Engineering, Polytechnique Montréal, C.P. 6079, Succ. CV Montréal, H3C 3A7 Québec, Canada

[b] Canada Research Chair in Intensified Mechano-Chemical Processes for Sustainable Biomass Conversion, Department of Chemical Engineering, Polytechnique Montréal, C.P. 6079, Succ. CV Montréal, H3C 3A7 Québec, Canada

KEYWORDS

CO_2, Formic acid, Fuel Cell, DFAFC, stack

ABSTRACT

Formic acid is a liquid, safe and energy-dense carrier for fuel cells. Above all, it can be sustainably produced from the electroreduction of CO_2. The formic acid market is currently saturated and it would require alternative applications to justify additional production capacity. Fuel cell technologies offer a chance to expand it while creating an opportunity for sustainability in the energy sector. Formic acid-based fuel cells represent a promising energy supply system in terms of high theoretical open-circuit voltage (1.48 V). Compared to common fuel cells running on H_2 (e.g., proton-exchange membrane fuel cells), formic acid has a lower storage cost and is safer. This review focuses on the sustainable production of formic acid from CO_2 and on the detailed analysis

of commercial examples of formic acid-based fuel cells, in particular direct formic acid fuel cell stacks. Designs described in the literature are mostly at the laboratory scale, still, with 301 W as the maximum power output achieved. These case studies are fundamental for the scale-up, however, additional efforts are required to solve crossover and increase performance.

1. Introduction

CO_2 accounts for over 80% of the global anthropogenic greenhouse gas (GHG) emissions that contribute to climate change [1]. Fossil fuel combustion is the largest contributor to the CO_2 released into the atmosphere. For instance, fossil fuel combustion represents over 75% of the total CO_2 emissions in the United States [2]. Transportation is the largest contributor to CO_2 emissions, with an estimated 15% share globally [3], with peaks over 30% for some countries, such as the United States. [2] After transportation, electric power, industrial and residential sectors are the ones with most CO_2 emissions [2].

A downstream CO_2 capture/conversion technology (CO_2 sink) would reduce the GHG concentration in the atmosphere. To sink CO_2 resulting from fossil fuel combustion, the first stage is CO_2 capture [4,5] and then either its storage [4] or conversion to fuels and chemicals [6–8]. A more or less appropriate approach to decrease CO_2 emissions depends on the sector and follow technological trends [9]. For instance, in the transportation sector, electrification [10] through plug-in hybrid electric vehicles (PHEVs) and plug-in electric vehicles (PEVs) equipped with efficient Li-ion batteries [11,12] seems the most viable short-term option. In the electric power sector, renewable energy feeding smart electricity grids in distributed energy generation (DEG) systems have the potential to replace traditional electricity power plants and decrease CO_2 emissions [13]. For the

industrial sector, process intensification (PI) technologies promise to decrease energy requirements from 20 to 80 % [14], with a corresponding reduction in GHG emissions [9,15].

Global sales of electric vehicles (EVs) expanded from less than 10,000 units in 2010 to 2.2 million in 2019 [16,17]. Breakthroughs in electrochemical energy storage technologies contributed to its rapid development over the last decade [16]. EVs have a huge potential market. Tesla and Nissan are established EV global players [18], while BMW [19] and Volvo [20] have committed to invest in electric cars and fuel-cell research. EVs are an environmental-friendly alternative to fossil fuel powered vehicles (especially when the electricity comes from a renewable source). Although EVs powered by Li-ion batteries dominate the market, issues concerning their energy storage capacity, safety and cost encouraged a shift towards alternative technologies such as fuel cells (FC) [16]. A FC requires a continuous source of fuel (chemical energy) and oxygen (or air) to sustain the redox reactions. FC technology prevents environmental pollution and provides environmentally friendly energy [21]. Furthermore, it offers practical benefits over batteries with high energy density and requires only 5 to 10 minutes for a full recharge [22,23]. FA is a candidate fuel for FC applications that may in turn be produced from CO_2, thus also contributing decreasing greenhouse gases in the atmosphere.

Electrochemical reduction can convert carbon feedstock into liquid fuels such as formic acid (FA) and alcohols. The CO_2 to FA transformation occurs in the presence of post-transition metal catalysts such as Sn, Pb, and Bi [24,25], but it occurs on Cu as well [26]. While there are various methods of storage and conversion to fuels and chemicals from CO_2, this review focuses on FA from CO_2 as a green feedstock for FC [6–8]. Despite the rise of electricity-driven technologies and the production of FA from green feedstock, the FA market is still limited and the demand is currently

saturated, unless new technologies requiring it reach commercial maturity. FA fuel cells (FAFC) will likely be one of these technologies. FA is a small molecule that does not require storage at high pressure and it feeds directly the FC, without the need for a catalytic reforming unit [27]. Since FA represents a form of carbon-based energy from CO_2 and H_2, it is an ideal feedstock for FCs to produce electricity and reduce environmental impact. Specifically, direct FA fuel cells (DFAFC) are attractive for small portable FC applications and promising for automotive batteries by vehicle electrification [28–30]. DFAFC have the potential for a carbon neutral cycle where CO_2 is first captured and then transformed into FA through an electrolyzer (Figure 1). Afterwards, FA is used in the FC to generate electricity and power vehicles, reemitting the previously captured CO_2. The carbon neutrality of this cycle clearly depends on leveraging renewable sources to produce electricity (e.g., photovoltaic, wind, hydro-electricity, etc.).

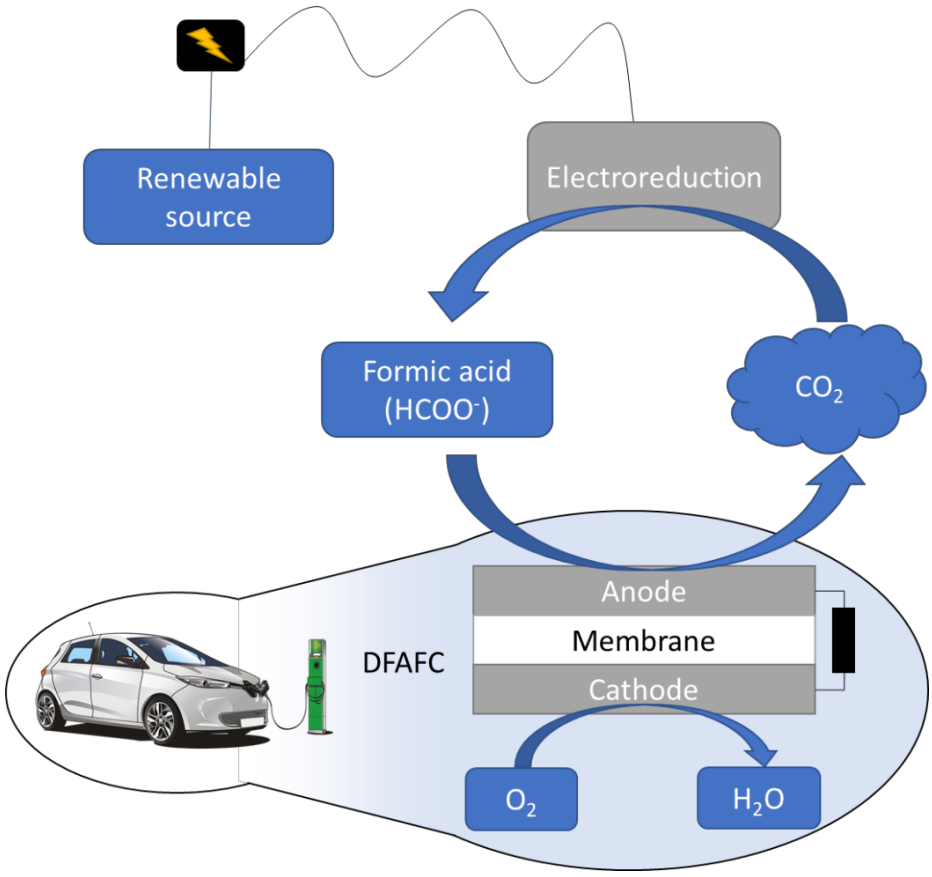

Figure 1 Simplified life cycle of CO_2 through an electroreduction unit and a DFAFC.

In 2009, Yu and Pickup reviewed the state of the art on DFAFC, focusing on anodic catalysts, and fuel crossover through Nafion© membranes [30]. They point out that micro-FCs have a greater commercial potential than conventional batteries as they deliver more energy per volume and weight [30]. In another review, Rees and Compton cover DFAFC with an emphasis on anode and cathode materials, and fuel crossover relative to membranes, where fuel crossover causes the fuel to move from the anode to the cathode [31]. They concluded that the available catalysts either had high performance and short longevity or vice versa, with one of the main aspects deactivating them being acid corrosion and poisoning by CO and by-products [31]. Since 2011, new literature data on DFAFC and innovative technologies have become available. Soloveichik reviewed liquid direct FC, including alcohols, FA and other fuels [32]. In 2017, Fukuzumi's evaluated the photocatalytic production of different solar fuels (methanol, formaldehyde, and FAs), and the theory and chemistry behind their application in FC [33]. All the reviews cited above, agree on the potential of DFAFC as portable electronics in a not too far future, mainly due to their limited fuel crossover, and high-power densities at low temperature.

In this review, we examine the potential of FA production from CO_2, targeting the progress in the field of DFAFC since Rees and Compton's 2011 review. This review presents the trending choices for anode and cathode materials, and the scale-up efforts of DFCAFC in the form of electrolytic stacks, which the literature has not yet covered. We also present the major issues limiting the spread of this technology and the impact on FA market, as well as the options in terms of FCs technology.

2. CO_2 electroreduction to formic acid

FA is typically produced by the reaction between methanol and CO in the presence of a strong base, followed by methyl formate hydrolysis [34], hydrolysis of formamide, and acidolysis of formate salts [35]. The production of FA from renewable sources, either from biomass [36] or from CO_2 brings environmental benefits while reducing our dependence on fossil fuels [37].

$$CO_2 + 2H^+ + 2e^- \rightarrow HCOOH \text{ (Eq 1 [38])}$$

In CO_2 electroreduction, cell conditions are neutral to alkaline in most cases, and formate ($HCOO^-$) is thus produced. Lowering the pH then generates FA. Several papers refer to FA, while they actually produce formate. The conversion of formate to FA is unrelated to electrochemical performance. For simplicity, we will refer to "FAFCs" herein.

Most literature data on the CO_2 electroreduction refer to H-cells (simplest devices for quick electrochemical tests, so called for the typical H-shape). However, from an industrial standpoint, there is a growing interest in flow cells mostly because of increased mass transfer [39]. Several H-type and flow cells from literature report Faradaic efficiencies of more than 80 % for large current densities (Table 1).

Table 1 Examples of recent CO_2 electroreduction.

Catalyst	Electrolyte	Potential (V vs RHE)	Faradaic efficiency toward FA (%)	Current density (mA/cm^2)	Reference

Nanotube derived - Bi	0.5 M $KHCO_3$	-0.61 V	100	288	[40]
nBuLi-Bi	Porous solid electrolyte	-0.77 V	97	450	[41]
Ultrathin Bi nanosheets	0.5 M $NaHCO_3$	-1.5 V	95	11	[25]
Sulfur-doped indium	0.5 M $KHCO_3$	-0.98 V	93	~60	[42]
Chain-like mesopourous SnO_2	0.1 M $KHCO_3$	-1.06 V	95	13.6	[43]
Sn nanoparticles (commercial)	Catholyte-free and 1 M KOH anolyte	-0.2 V	93.3	51.7	[44]
Bi-PMo nanosheets	0.5 M $NaHCO_3$	-0.86 V	93	30	[45]
Electrodeposited Bi dendrites	0.5 M $KHCO_3$	-1.0 V	92	38.1	[46]
Boron-doped Sn	1 M KOH	-0.72 V	91	65	[47]
Bi/C nanoparticles	1 M KOH	-	89.2	45	[48]
Sn-based	0.1 – 1 M $KHCO_3$	-	90	~30	[38]
Carbon supported SnO_2	0.4 M K_2SO_4	-	90	500	[49]
2D-Bi	Deionized water (solid electrolyte)	-0.79 V	90	30	[50]
Sn/SnO_x	0.1 M $KHCO_3$	-1.2 V	89.6	11.2	[51]
Sn plate	0.1 M Na_2SO_4	-1.35 V vs SCE	82.5	-	[52]

Sn plate	0.125 – 0.5 M K_2SO_4	-	80	~30	[53]
Tin (Sn) oxide - C	Deionized water only	-	80	200	[54]

Previous relevant works are presented by Han et al. [55]

H-cells are an appropriate set-up to screen and compare catalysts. However, there are several issues preventing the scalability of the system, i.e. poor solubility of CO_2 in water and aqueous electrolytes, as well as limited diffusivity towards the electrode. Between 2007 and 2017, more than 1,000 research articles report catalysts analyzed on H-cells; however, only 21 articles report on flow cells for CO_2 reduction [56]. Commercially-viable systems to convert CO_2 to FA require current densities of at least 200 mA/cm^2 stable over time [56] and higher for more compact electrodes, driving the overall electrolyzer cost down, whereas Faradaic efficiency, which can reach 90%, are less of a limiting factor for commercial applications. Like water electrolyzers, industrial CO_2 electrolyzer systems consist of stacked flow cells. Some literature examples report lab-scale cell designs that allow a systematic scale up, i.e. membrane-based and microfluidic flow cells [56]. Both of these cells attain current densities beyond 200 mA/cm^2 at the laboratory scale. This threshold is suitable for commercial applications, however, when scaling fuel cells up, it is uncertain that current density will scale linearly, and achieving higher density at the lab scale is required to accelerate their market adoption. Strategies to further improve the current density consist of (1) modifying the electroreduction cell geometry and/or reactor design (i.e. electrodes configuration) in continuous or discontinuous configurations for liquid electrolytes to flow between the electrodes, increase both energy and current efficiency [57], and (2) increase CO_2 solubility with non-aqueous electrolytes [58]. In the first case, the cathode electrode can be placed at the interface between the electrolyte and the gaseous CO_2 for enhanced mass transfer [59]. As such,

pressure equilibration between the liquid electrolyte and the gaseous CO_2 need to be ensured to prevent products crossflow through the porous electrode.

The reactor design is a critical step that must be considered in concomitance with new catalyst development to meet high current and energy efficiencies[57]. Zero-gap assembly of gas diffusion electrodes maximizes energy efficiency but inhibits CO_2 reduction, while introducing a thin liquid buffer layer between the cathode and the membrane to achieve high current efficiencies[57]. Another recent comparison was presented by Diaz-Sainz et al., where gas diffusion electrodes and catalyst coated membrane electrodes are compared for Sn and Bi-based materials [48]. In terms of material choice, Bi-based configurations outperform the Sn-based ones, while in terms of electrodes design gas diffusion electrodes present lower performance in terms of formate concentration and energy consumption [48]. Several techno-economic analyses on the electroreduction of CO_2 to FA show that the process is economically viable despite the large consumption of electricity [60]. Agarwal et al. propose a scenario under which CO_2 flow cells could be economically viable. This scenario includes an electricity consumption of 5.2 MWh/ton of generated FA with an electricity cost of 0.07 US$/kWh. It also comprises the condition of CO_2 provided at no cost and FA being the feedstock for high value applications, such as H_2 storage or chemical feedstock.[60]. Although electrochemical reduction of CO_2 to FA is both technically and economically feasible, technical challenges remain an obstacle to commercialization, namely the needs of high overpotential, cathode stability as well as the integration of high steam consumption in final separation and CO_2 capture at ambient temperature and pressure [61]. Finding new applications and markets for FA will incentivize the development of CO_2 electrolyzers and make FAFCs pertinent for CO_2 electroreduction.

3. Formic acid market

In the 2014-2019 period, the worldwide production of FA fluctuated between 750,000 – 800,000 tons [34,62]. The total trade value of FA in 2018 was $430 million [63]. The predominant markets for FA demand are Asia and Europe (48% and 36% share, respectively) [64]. FA sold at a concentration of 85% is the global industry standard, but special applications require a concentration of 99% [64]. The historic use of FA for leather hide tanning has decreased over the past 20 years due to the leather industry shrinking. Pharmaceutical production, food industry, textiles, drilling fluids, and airport runway deicers, natural rubber, chemicals, and animal feed account for the remaining consumption [64].

IHS Markit reported that the market of FA is amply supplied [64]. Silage preservation/animal feed additives and leather and tanning account for nearly 49% of world consumption [64]. As a result, these applications define demand-driven growth. Consumption in silage preservation and animal feed additives have benefitted from the continuously improving living standards (particularly in Asia) and the increasing meat consumption [64]. The lower labor and capital costs, as well as the rapidly growing market will allow China to increase FA capacity; China will remain the single-largest producer and exporter of FA [64].

FA's price also affects its application in fuel cells (Figure 2). Between 2011 and 2013, FA reached its highest price (over $1100). Afterwards, the Chinese market crash of 2014 affected the FA market price until 2017. Between 2017 and 2019, the price of FA increased at around $ 700. However, the COVID-19 outbreak has almost halved the price. A recent FA market forecast predicts a revised compounded annual growth rate of 3.3%, accounting for US$ 363.4 million [65–67].

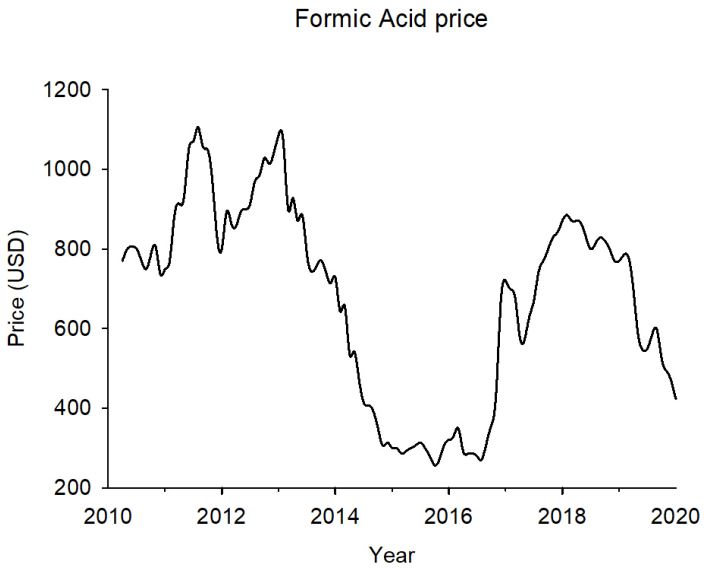

Figure 2 China's market price of FA (94%) from April 2010 to April 2020 [68].

4. Formic acid fuel cells (FAFC)

4.1 Fuel cells

A fuel cell is a device that generates electricity from chemical energy. The electrolyte determines the operating temperature and fuel type [69]. Depending on the electrolyte type, there are solid oxide fuel cells (SOFC), molten carbonate fuel cells (MCFC), alkali fuel cells (AFC), phosphoric acid fuel cell (PAFC) and proton exchange membrane fuel cell (PEMFC). SOFC uses a hard, ceramic material (oxides of calcium, zirconium, etc.) as the electrolyte. In SOFC temperatures reach 800 – 1000 ^{o}C, leading to a voluminous fuel cell unit and an increased risk of cracking [70]. In an MCFC, salts (Na or Mg) facilitate the movement of carbonate ions [71]. Despite advantages such as variable fuel options, resistance to impurities, the high temperatures required limit SOFC and MCFC when portability is one of the characteristics desired [72].

AFC have historical relevance, being the primary electrical source in the Apollo space program. AFC operates on pure compressed H_2 and O_2 with expensive Pt electrode catalysts [73]. AFC technology leverages a wide range of electrocatalysts, such as Ni, Ag, metal oxides, and noble metals [74]. Their operating temperature ranges from 150 to 200 ºC and cell output ranges from 300 W to 5 kW with an energy efficiency of 70 % [75]. AFC is sensitive to CO_2, requiring thorough purification of H_2 from CO_2 [75]. Concentrated KOH or NaOH serves as the electrolyte, presenting a chemical hazard risk in case of leakage [75].

Phosphoric acid is an ion-conducting electrolyte that forces electrons to travel from the anode to the cathode through an external electrical circuit. The working temperature for PAFC is between 150 to 200 ºC, and cell output can be up to 200 kW with an efficiency between 40 % to 80 % [76]. Drawbacks of PAFC's include its reliance on hydrocarbons, the high cost of Pt catalysts and rather low power density [77].

PEMFCs are considered competitive candidates to substitute batteries for EVs [30]. A proton-conductive polymer membrane (typically Nafion®) separates the anode and cathode. The operating temperature is about 40 – 100 ºC and the cell output ranges from 50 kW to 250 kW with an efficiency of 40 – 50 % [78]. Commercial PEMFC utilize H_2 But the need of pressurizing it up to 700 bar for storage and transport translates into the need of particular infrastructure to ensure safe storage and refilling by vehicle users. H_2 cost is estimated at an average of 2.6-5.1 US$ per kg [79,80] (comparing to FA of ~0.7 US$ per kg in 2017-2019, Figure 2). Since FCEV are 2.5 times more fuel-efficient than gasoline, a gallon of the latter needs to be 2.5 times less expensive than a kilogram of H_2 to keep the same cost per mile [81].

Compared to H_2-fed fuel cells, direct liquid fuel cells (DLFCs) are easier to handle, store and transport [82]. Alcohols [21], such as methanol [83], ethanol [84] and ethylene glycol [85], are the most common liquid fuels. Methanol has excellent energy density (~4900 Wh/L), but is toxic and it has a high rate of fuel crossover at high concentration [86]. The oxidation of ethanol is slow since it involves a 6-electron reaction [87]. Ethylene glycol as a fuel and hydrogen peroxide as an oxidant in alkaline fuel cells may help overcome the issue of carbonate formation when CO_2 in the air reacts with OH^- to form CO^{3-} [88].

FA is a promising fuel for DLFC over alcohols, because of lower fuel crossover, higher theoretical cell potential and power densities, as well as faster oxidation kinetics when compared to alternative options [30]. This work focuses on FA FCs, where electrochemical reduction of CO_2 produces the feed.

We provide a comparison of cost, energy density, operating temperature, energy density and pressure storage of some fuels. We selected these fuels as they can be produced from renewable sources (FA and alcohols through CO_2 reduction; H_2 through electrolysis with renewable electricity; gasoline from biomass or gas to liquid processes starting either from CO_2 or biomass) When compared to H_2 and methanol, which are commonly used in fuel cells, FA requires milder operating conditions, has a higher energy density than H_2 and is inherently safer than methanol Gasoline is unrivaled as a fuel considering the energy density. However, producing gasoline from either biomass or CO_2, involves multi-step, high temperature processes, whereby carbon losses and emissions are more likely than in electricity-driven technologies [89,90](Table 2).

Table 2 Comparison of fuels price, energy density, operating temperature and storage pressure.

	Fuel	Price (retail)	Energy density	Operating Temperature	Storage Pressure
Fuel Cells	FA	0.7 US$ / kg [68]	2.1 kWh dm^{-3} [91]	20-60°C (DFAFC) [87]	-
	H_2	2.6-5.1- US$ / kg [92,93]	0.53 kWh dm^{-3} [94–96]	150-200°C (AFC) [75]	700 bar [81]
	Methanol	0.2-0.4 US$ / kg (China) [79,80]	4.4-4.9 kWh dm^{-3} [96,97]	30-90°C (DMFC) [98]	-
	Gasoline	0.6-2.3 US$ / gallon [99]	13 kWh dm^{-3} [100]	-	-

4.2 Direct formic acid fuel cell

DFAFC are a technology characterized by relatively easy power system integration, low toxicity, and stability compared to other fuel cell types [101]. FA crossover flux through Nafion® membrane is low because the repulsive force between formate anions and ion clusters enhances the compatibility with membranes. Moreover, they are characterized by a theoretical electromotive force of 1.48 V (1.18 V for methanol) and an energy density of 2.11 kWh dm^{-3} (4.4 kWh dm^{-3} for methanol) [96,97]. As a reference, H_2 fuel cells (FCs) have an electromotive force and energy density of 1.23 V and 0.53 kWh dm^{-3} [94–96].

4.2.1 Reaction mechanism of DFAFC

DFAFCs operate on the same principle as other FCs. They generate electric energy from FA oxidation and O_2 reduction. In the electrochemical device, FA and O_2 (or air) are fed to the anode and the cathode, respectively. An electrolyte membrane allows the protons to flow [97] (Figure 3).

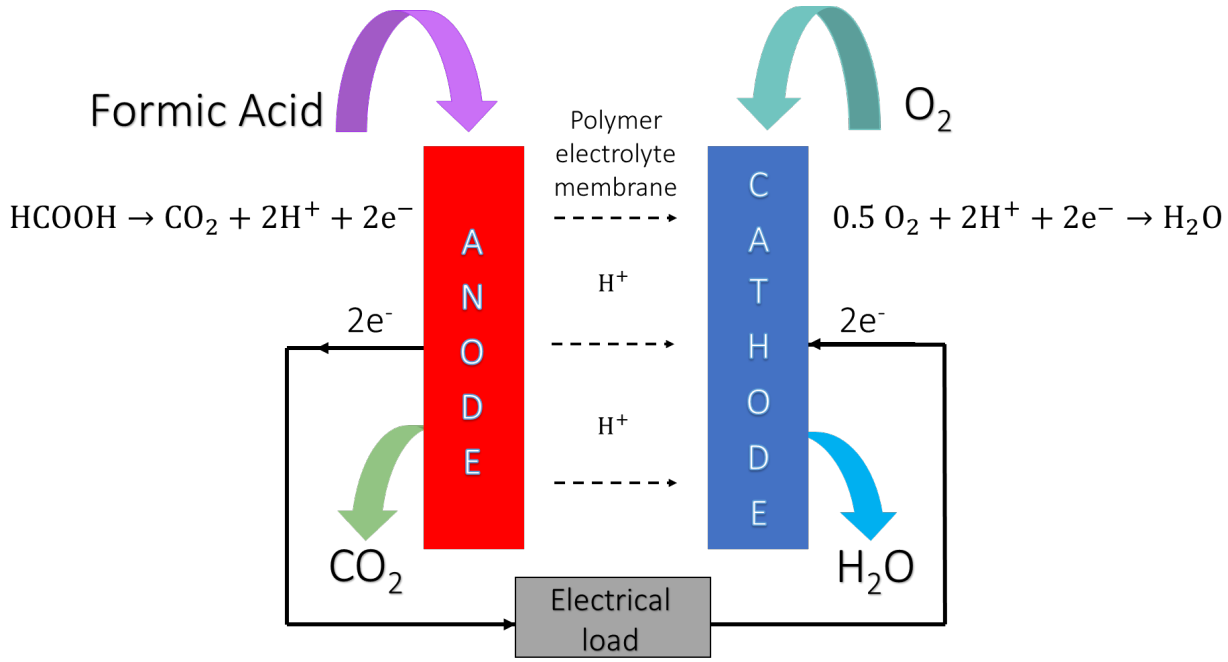

Figure 3 Direct formic acid fuel cell (DFAFC) scheme.

The direct anode, cathode and the overall reaction of DFAFC are as following [30]:

$$HCOOH \rightarrow CO_2 + 2H^+ + 2e^- \quad \text{(Eq 2)}$$

$$0.5\ O_2 + 2H^+ + 2e^- \rightarrow H_2O \quad \text{(Eq 3)}$$

$$HCOOH \rightarrow CO_2 + H_2O \quad \text{(Eq 4)}$$

The indirect anode reaction:

$$HCOOH \rightarrow CO_{ads} + H_2O \rightarrow CO_2 + 2H^+ + 2e^- \quad \text{(Eq 5)}$$

At the anode, the direct FA oxidation proceeds via decomposition (Eq 2) [21]. In the ideal direct pathway, HCOOH → *HCOO (formate) or *COOH (carboxyl) then completely transforms into H_2 and CO_2 [103]. In the indirect dehydration of FA (Eq 5), HCOOH → *COOH → *CO → CO_2, the undesired CO could poison the catalysts by interacting with the active sites, thus increasing the required overpotential for oxidation [21]. Experiments [104–108] and theoretical studies [103,109–111] attempted to suggest the reaction mechanism. The pathway of FA oxidation depends on the nature of the catalyst, like the pH at the anode/electrolyte interface [103]. For example, the electrooxidation current of HCOOH/$HCOO^-$ on a Pt catalyst exhibited a maximum oxidation current at a pH of 3.75 over a pH range of 0-12, close to the pKa of FA [107].

4.2.2 Anode catalysts

Anode catalysts with high reactivity and durability are essential for DFAFC [112–116]. Platinum (Pt) and palladium (Pd) based catalysts are two prominent anode options for DFAFC [103,117].

Weber et al. first introduced Pt as an electrode in 1996 [118]. They demonstrated that Pt/Ru catalyst is more active than Pt-black in FA oxidation. Pt electrode surfaces influenced the reaction path: on the steps and terraces of Pt nanoparticles, the FA oxidation proceeds via the direct pathway; differently, on plain Pt nanoparticles it occurs via the indirect pathway [119,120]. Voltammetry studies showed that Pt (111) suffers of poisoning [120–123]. There are however difficulties to mass-produce Pt nanoparticles with controlled shape [119].

As an alternative, Pd catalysts present better CO tolerance and higher power density than Pt-based catalysts [124,125]. Pd also catalyzes FA to CO_2 primarily via the direct pathway [103,117]. However, the agglomeration of Pd particles and the accumulation of CO on Pd surfaces promote the design and

synthesis of nanoparticle catalysts with large superficial areas with 3D porous or hollow structures [126–128]; and the introduction of a more oxyphilic metal, such as Ni [129], Co [130], Cu [131], and P [132], to form OH*, which oxidizes CO* to CO_2 [102].

DFAFC performance improves when Pt or Pd form alloys with metals such as Pb, Sn, Au, Bi, As, and Sb [133–139] or their surface is modified [140–142], such as by irreversibly adsorbing a second metal [119].

Carbon nanotubes or expanded graphite layers as supporting material reduces the loading of noble metal and improves the electrical conductivity and stability of Pt or Pd catalysts [143]. Other supporting materials include titania [144], zirconia [145], V, Mo, W and Au [123], and tungsten carbide [91,146].

4.2.3 DFAFC stack designs

PEMFC stack design principles

The heart of a fuel-cell system is the membrane electrode assembly (MEA, includes the proton exchange membrane, and the anode and cathode catalyst layers and gas diffusion layers (GDLs) on each side of the membrane) [147]. A single cell resembles a sandwich with a MEA, sealed with gaskets to prevent gas leakage, between two separators or bipolar plates. The potential of a single FC decreases during the operation as a function of current density [148]. Individual cells are stacked to achieve the voltage, current or electric power for industrial generators or automobiles [119]. Increasing the number and the area of the MEAs raises the voltage and the output of the stack [119]. A commercial H_2 FC stack, acting as a tiny electric power station, consists of hundreds of single

cells, like slices in a loaf of bread [149]. Other components include current collector and end plates. The whole stack is tightly held in place by tie-rods, bolts, shrouds or other arrangements [148].

A typical PEMFC works as follows: air and fuel (H_2 source) are fed to the bipolar plates and flow into the channels of the plates; H_2 diffuses through the GDL, contacts the anode catalyst layer and is then split into protons H^+ and electrons e^-. Electrons pass through the GDLs, the bipolar plates, the current collectors and arrive at the cathode via an external circuit. O_2 reduces to water as a by-product with the protons H^+ passing through the membrane [150]. The MEA acts as a barrier for electrons, creating a flow of direct electrical current in the external circuit [150].

Other than bipolar configurations, ideal for large fuel cells, there are also side-by-side configurations such as zig-zag or flip-flop connections that increase the fuel concentration at the anode by order of magnitudes compared to other arrangements [148].

The main key features for the design of a stack include:

- Uniform distribution of the reactants to each cell by an external or internal parallel manifold: the flow pattern can be "U" shaped (inlet and outlet are at the same side but in opposite direction) or "Z" shaped (inlet and outlet are at different side). Alternatively, a parallel-serial manifold has the depleted gas flow from the first "Z" shaped segment to the next cell [148]. The latter operates at higher stoichiometry [151].
- Uniform distribution of reactants inside each cell by selecting the shape of the flow field (square, rectangular, etc.); flow field orientation (top to bottom, bottom to top, side to side, etc., considering water condensation); channel configuration (straight, criss-cross,

single/multi-channel serpentine, mesh, porous, etc.); channel shape, dimensions and sizing [148].

- Cooling system with coolant (between or at the edge of the cells), phase change material, or reactant air itself [148].
- Proper clamping force to prevent leakage (depending on the gasket material and design) and diminish contact resistance (1.5 - 2.0 MPa) [152].

DFAFC stack examples

A FC stack includes repetitive, simple geometry cells [148]. Despite most research focuses on the choice of anode catalysts, a FC's performance does not depend only on the anode's and cathode's catalyst, but also on the membrane, gas diffusion layers, hardware, stack design, etc. [119]. The selection of key parameters and operating conditions affects the whole stack performance, which is crucial for industrial applications. Examples of practical devices for DFAFC stacks are not abundant in the literature, but each stack has a distinct design and has been tested under optimal operation conditions, providing insights for further study (Table 3).

Table 3 Catalysts and performances of DFAFC stacks reported in literature.

Number of stacks	**Air breathing type**	**Anode catalyst**	**Cathode catalyst**	**Maximum power density (mW cm^{-2})**	**Power output (W)**	**Reference**
15 MEAs	Active	Pt-Ru (Johnson Matthey)	Pt black (Johnson Matthey)	60	30	[153]
2 MEAs	Passive			44.5	0.4	[87,154]

4 MEAs		40 wt.% Pt/C (Johnson Matthey)	40 wt.% Pt/C (Johnson Matthey)	56.6	0.9	
10 MEAs	Passive	60wt% Pt/C + 60wt% Pd/C (Pt-Pd/C)	60 wt% Pt/C	130	32	[155]
35 MEAs	Passive	40% Bi-modified Pt/C	Pt Black	191	301	[119]

DFAFCs classify into 1) active DFAFCs, where the liquid fuel is fed to the anode through a pump and compressed air to the cathode; 2) active air breathing DFAFCs, where the cathode is exposed to ambient air; 3) passive air breathing DFAFCs [156], whereby there are no pumps and/or compressors metering fuels and/air to the cell, which makes them compact and portable.

Miesse et al. [153] were the first to report an active DFAFC stack in 2006, which is capable of 30 W at 60 mW/cm^2 to power a laptop computer over 150 mins. The MEAs were separated by bipolar plates (Figure 4, Table 3). The packed stack includes a fuel tank, tubing, a miniature liquid fuel pump and an air compressor, and a power conditioning control board (PCB). It is a hybrid system, as there is a small battery to drive those components during start-up. They were able to operate at 50 % by weight of FA. Together with the work Zhu et al. [157], who adopt FA concentrations between 1M and 12M, the data from Miesse et al. are the ones gathered at the highest FA concentration in the literature, which is key for industrial applications. Indeed mass-transfer limitations and crossover [158,159] seem to occur consistently at concentrations < 3M and > 6M, respectively. In the work by Miesse at al., the flow field orientation also affected the stack performance: feeding FA

from the bottom to the top of the stack avoided CO_2 accumulation. Poor distribution of FA in the cells resulted in an earlier onset and downward trend of the polarization curve, which translates into decreased performance. Dynamic response reflects the stack response to the demand change of the electronic devices, and also determines the need for supplementary equipment [153]. The transient response showed that this 15 MEA stack reacted to a step change in current and power with no power lag. This stable long-term performance is key for commercial feasibility. Miesse et al. conducted a three-month continuous operation on a single cell MEA. Steady state was reached after several hundred hours of operation (degradation <15%). Furthermore, applying a high anodic potential to the catalyst re-establish the anode activity once lost [124]. Based on this study, Miesse et al. suggested a cell or stack cycling to recover decreased performance. A circulating fuel loop, a sensible pH meter, or an electrochemical sensor is recommended to monitor the continuous decline of FA concentration inside the tank during operation.

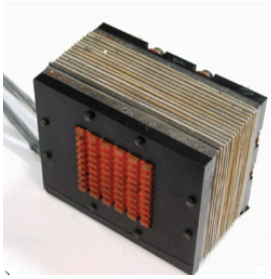

Figure 4 Stack with 15 MEAs in series, 88mm×70mm. Air and FA was fed to each MEA in parallel through internal manifolds. The graphite-composite bipolar plates (1.5 mm pitch) had square-grooved, parallel, serpentine flow fields. Reproduced with permission from [153].

Passive FCs are lighter and smaller compared to active ones with auxiliary equipment (e.g., liquid fuel pumps and air fans). Hong et al. designed a passive air-breathing two-cell stack [154] and four-

cell stack [87] DFAFC. The two-"face-to-face"-cell stacks shared one fuel reservoir. The design of two-cell and four-cell stacks was similar (four-cell stack as an example: Figure 5a). FA has high electrical conductivity properties, and water electrolysis can readily occur when over three cells sharw one fuel reservoir [154,160]. In the four-cell stack, Hong et al designed a fuel reservoir with four independent cavities for individual cells (Figures 5b). This design avoids water hydrolysis between electrodes [87]. The four-cell stack was assembled with gold coated printed circuit boards as end plates and current collectors (Figure 5c). The MEA were prepared by direct catalyst spraying [161]. The performance of each cell is uniform according to the overlapping curve of the open-circuit voltage. The optimal concentration of FA in this work was 5M. The transient response of each cell under a step change in current had a relatively stable voltage. The stack and each single cell showed similar "fast-slow-fast" degradation pattern, thanks to the symmetrical stack design; ~20 % of the stack voltage dropped during the 10 h long term performance test due to the deactivation of the catalysts and of the MEA. The authors specifically mention the limited fuel supply and its consumption in the reservoir as a matter to investigate further.

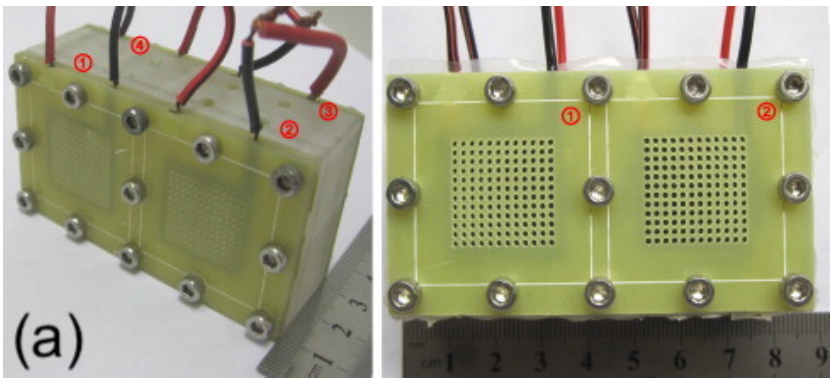

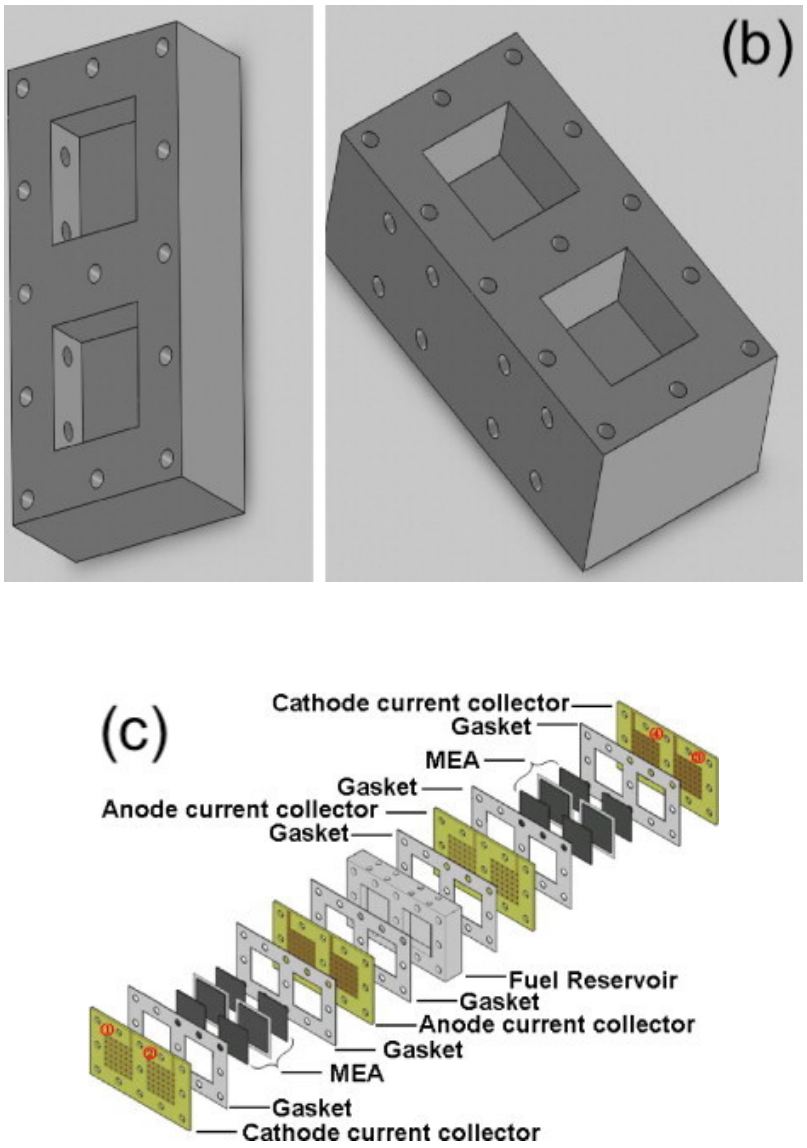

Figure 5 (a) Passive air-breathing DFAFC four-cell stack: 7.5cm×3.0cm×4.0cm. The anode of one cell is connected to the cathode of next cell. Two external wires are for the performance testing of each cell. (b) Left and right views of fuel reservoir (by AutoCAD): four cavities store the fuel and support individual cell. (c) Detail breakdown sketch of the four-cell stack [87].

Cai et al [155] designed and fabricated a medium-scale 10-cell (5 cm × 5 cm) DFAFC stack (Figure 6). The anode catalyst was 60 wt% Pt/C + Pd/C catalyst synthesized in laboratory, mixed by

ultrasound and sprayed on the wet-proof carbon papers. The MEA was formed by two electrodes with a Nafion© 117 membrane via hot pressing. The bipolar plates are graphite with serpentine channels on both sides. Under optimal operation conditions (10 mol L^{-1} FA solution and 2.0 L min^{-1} O_2), the power output of this stack reached 32 W, suitable for most portable electrical devices. The stack can stably operate for 50 h with 1.5 L fuel and up to 240 h (with refueling) with no decline of performance. Furthermore, by washing the anode catalyst significantly increased the maximum power output 60 % higher than the unused stack.

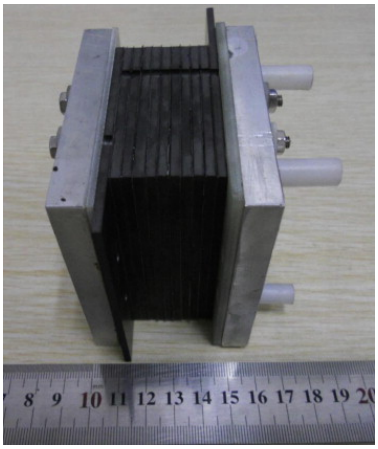

Figure 6 The DFAFC 10-cell stack with bipolar graphite plates [155]

Most stacks employ commercial catalysts. Choi et al. [119] prepared an irreversibly adsorbed Bi on Pt/C catalyst to prevent the Pt catalyst from CO poisoning and applied it in the stack. Adding Bi formed Pt ensembles which favored the direct oxidation of FA and thus decreased CO production. A high loading of Bi covers the dehydrogenation Pt sites; hence, a coverage of 0.25 was a good compromise. The O_2 reduction reaction rate was lower compared to commercial Pt/C catalysts. Yet, the FA oxidation activity of the Bi-Pt/C catalyst was 13 times higher than Pt/C at 0.58 V. The authors applied this catalyst to a DFAFC stack of 35 membrane electrode assemblies (MEAs). MEAs fabrication followed a catalyst-coated membrane method. A manual air-brush system (GP2,

Japan) directly sprayed the anode and cathode layers on both sides of the membrane (NR212). Figure 7 displays the fabricated DFAFC stack with Bi-Pt/C catalyst. 35 MEAs are stacked, each with a geometric area of 50 cm^2 and the maximum power is 301 W. The cell that performs the worst determines the overall performance, and usually is the main cause of performance degradation of the stack [87]. In this case, most cells have similar single cell performance. Three cells close to the anode have relatively poor performance, probably because of insufficient air or liquid fuel supply [162].

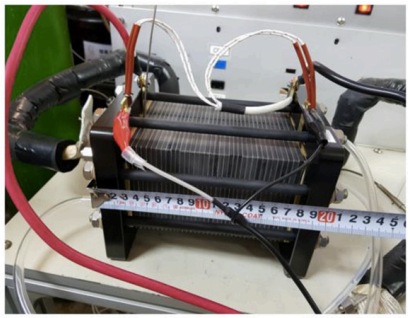

Figure 7 300 W DFAFC stack includes MEAs, GDL, gaskets and bipolar plates (15.6cm×11.6cm×9.8cm) [119]

4.2.4 Status, challenges and opportunities

DFAFCs stacks are still limited to the laboratory scale, with typical power outputs from below the unit to ~30 W, with an outlier of ~301 W (Table 3). Most catalysts under investigation in the literature are commercial catalysts, except the one from Choi et al. [119] who tested Bi-modified catalysts. Stack geometries and experimental conditions are similar with FA concentrations ranging from 2 M to 12 M and temperatures between 20°C and 60°C, with the exception of Hong et al. who developed their four-cavity geometry [87]. Data indicate that FA concentrations at 5-6 M lead to higher power densities with optimal temperatures at 60°C. The superior performance from

Choi et al. advocates for the development of new efficient catalysts [119]. More data on DFAFC stacks will help identify optimal working conditions, including FA concentration and flow rate, air flow rate, and cell temperature. Up to now, there are no commercial DFAFC devices. Comparatively, Horizon Fuel Cell Group [163] built a liquid-cooled H_2 FC that has been implemented in around 10 buses and trucks, with a power output ranging from 60 to 150 kW. They plan to produce the world's highest power PEMFC with 300 kW stacks by 2020 [164].

Challenges for commercial DFAFCs that remain to tackle include the crossover of FA through Nafion© membranes (fuel permeates the membrane from anode to cathode, a common issue for PEMFC). Kim et al. reviewed the characterization techniques (stand-alone membranes and MEA configurations) of FC membrane [165]. The chemical structure and operation conditions of PEMs greatly affect the ion exchange capacity, water uptake, ion conductivity, gas/liquid permeability and chemical/physical stability [165]. Although FA has a low crossover through Nafion©, it still affects the performance of DFAFCs [123]. Increasing FA concentration and operating temperature raises the risk of crossover [166]. The choices and preparation of the gas diffusion layer, catalysts and MEA also cause the crossover problem. Hence further studies are needed to improve the performance of DFAFCs.

4.3 Pre-commercial indirect formic acid fuel cells

There are examples in the literature of indirect FAFCs where FA plays the role of H_2 source. An indirect FAFC is a fuel cell whereby the feed is FA, but the fuel is H_2 being stored in it. It combines the advantage of having FA as a liquid feed, which is easy to transport and store vs. H_2. Indeed this latter must be stored and transported under pressure, besides carrying higher safety concerns. Team FAST, a student-run project at the Technical University of Eindhoven in the Netherlands,

designed the world's first electric-powered bus based on Hydrozine (99% of FA and 1% of an undisclosed performance enhancing agent) [167]. Hydrozine is sustainably produced from the electrochemical reduction of CO_2 by VoltaChem [168]. The system transforms the Hydrozine into CO_2 and H_2, which is then sent to a FC to produce electricity in a closed carbon-loop [169]. In 2014, Pico, a device driven by Hydrozine, was developed for the first time [169]. In 2015, Team FAST created a scale model, Junior, which works on Hydrozine and has a maximum speed of 70 km/h. In early 2016, Team FAST built their current system, REM, with an output of 25 kW thought to power electric buses [167]. REM is still a prototype and the FC suffers from issues such as temperature control and unstable electrical power [170].

Being FA a very efficient H_2 carrier (1 L FA carrying 590 L H_2), it makes H_2 easier to store and transport in a liquid form to feed into a conventional H_2FC [171]. In 2018 GRT group [172], a company focused on energy transition with energy-storage development solutions, and the Laurenczy group from EPFL [173] developed the world's first integrated FA-H_2 FC device. The device consists of two main parts, a H_2 reformer (HYFORM) to extract H_2 from FA and a proton-exchange membrane fuel cell (PEMFC). FA is produced from biomass or through the hydrogenation of CO_2 and is stored at room temperature in a tank. The HYFORM uses a Ru-based catalyst to transform FA into H_2. H_2 then passes through the FC to produce electricity. Excess CO_2 can be recycled to produce FA. The HYFORM-PEMFC has a capacity of 7000 kWh per year with an electrical efficiency up to 45%, and its theoretical power is 800 W. This design claims a 100% closed CO_2 loop and absence of particles and nitrogen oxides [174].

5. Conclusion

This manuscript reviews the latest advances in formic acid fuel cells (FAFCs) where CO_2 represents the suggested feedstock for FA. The market for FA is currently saturated but the increasing demand for electricity-driven devices brings interest in the development of FA fuelled FCs for a sustainable energy supply solution.

Literature examples with Faradaic efficiency of above 80% are many, whereby increasing current density beyond 200 mA/cm^2 is the main challenge for commercial applications for CO_2 to FA. However, the increasingly performing cells reported in the literature are encouraging the transition towards industrial scale cells for CO_2 electroreduction to FA.

The DFAFC stacks examples presented in this manuscript represent important milestones for the future development of prototypes, scale-up and commercialization. Stack examples have a number of membrane electrode assemblies (MEA) ranging from 2 to 35, with consequent power outputs ranging from 0.4 to 301 W. Commercial FAFCs face challenges to directly apply FA as a fuel, and future works need to tackle direct formic acid fuel cells (DFAFC) issues such as the crossover (fuel crossover causes the fuel to move from the anode to the cathode) deriving from high FA concentrations that are necessary in commercial FC.

Another application for FA relies on extracting H_2 from it in a reforming step and use this latter in a conventional H_2 FC (or indirect FA fuel cell). Indeed, FA is a very efficient H_2 carrier (1 L FA carrying 590 L H_2), which makes H_2 easier to store and transport in a liquid form to feed into a FC. Renewable carbon feedstock such as CO_2 or biomass is once again the recommended raw material to produce FA.

Further developments are looking at testing novel materials as catalysts and surveying new FC stacks designs to improve the power output of DFAFCs and overcome the performance of available commercial catalysts.

AUTHOR INFORMATION

Corresponding Author

***Daria C. Boffito -** [a] Department of Chemical Engineering, Polytechnique Montréal, C.P. 6079, Succ. CV Montréal, H3C 3A7 Québec, Canada; [b] Canada Research Chair in Intensified Mechano-Chemical Processes for Sustainable Biomass Conversion, Department of Chemical Engineering, Polytechnique Montréal, C.P. 6079, Succ. CV Montréal, H3C 3A7 Québec, Canada; https://orcid.org/0000-0002-5252-5752; * daria-camilla.boffito@polymtl.ca

Author Contributions

ZM lead the bibliographic research and drafted the manuscript. EP, UL and DCB performed the bibliographic research and drafted the manuscript. DCB also supervised the post-doctoral fellows involved and secured funding. JRT drafted the manuscript and supervised the post-doctoral fellows involved. All authors approved the final version of the manuscript.

Notes

The author Dr. U. Legrand is the CTO of Electro Carbon Inc., a company aiming to commercialize CO_2 to formic acid electrolysers and thus have financial interest in the present research. This conflict of interest did not influence the conclusions presented in the article.

ACKNOWLEDGMENT

This work was supported by Natural Sciences and Engineering Research Council of Canada (NSERC) and Sigma Energy Storage (SES). This research was undertaken, in part, thanks to funding from the Canada Research Chairs Program. The authors acknowledge the support of the National Research Council of Canada (NRC) for the support through the Materials for Clean Fuels Challenge Program.

REFERENCES

(1) Stocker, T. F.; Qin, D.; Midgley, P. M.; Plattner, G.-K.; Tignor, M.; Allen, S. K.; Boschung, J.; Nauels, A.; Xia, Y.; Bex, V. *IPCC, 2013: Climate Change 2013: The Physical Science Basis. Contribution of Working Group I to the Fifth Assessment Report of the Intergovernmental Panel on Climate Change*; Cambridge, United Kingdom and New York, NY, USA, 2013.

(2) EPA. *Inventory of U.S. Greenhouse Gas Emissions and Sinks: 1990-2018*; 2020.

(3) Rathee, S.; Kumar, A. Transportation Effects on Environment and Health Issues. *Int. J. Enhanc. Res. Sci. Technol. Eng.* **2017**, *6*, 101–106.

(4) Bui, M.; Adjiman, C. S.; Bardow, A.; Anthony, E. J.; Boston, A.; Brown, S.; Fennell, P. S.; Fuss, S.; Galindo, A.; Hackett, L. A.; Hallett, J. P.; Herzog, H. J.; Jackson, G.; Kemper, J.; Krevor, S.; Maitland, G. C.; Matuszewski, M.; Metcalfe, I. S.; Petit, C.; Puxty, G.; Reimer, J.; Reiner, D. M.; Rubin, E. S.; Scott, S. A.; Shah, N.; Smit, B.; Trusler, J. P. M.; Webley, P.; Wilcox, J.; Mac Dowell, N. Carbon Capture and Storage (CCS): The Way Forward. *Energy Environ. Sci.* **2018**, *11* (5), 1062–1176. https://doi.org/10.1039/C7EE02342A.

(5) Douïeb, S.; Archambault, S.; Fradette, L.; Bertrand, F.; Haut, B. Effect of the Fluid Shear Rate on the Induction Time of CO2-THF Hydrate Formation. *Can. J. Chem. Eng.* **2017**, *95* (1), 187–198. https://doi.org/10.1002/cjce.22650.

(6) Albo, J.; Alvarez-Guerra, M.; Castaño, P.; Irabien, A. Towards the Electrochemical

Conversion of Carbon Dioxide into Methanol. *Green Chem.* **2015**, *17* (4), 2304–2324. https://doi.org/10.1039/c4gc02453b.

(7) Artz, J.; Müller, T. E.; Thenert, K.; Kleinekorte, J.; Meys, R.; Sternberg, A.; Bardow, A.; Leitner, W. Sustainable Conversion of Carbon Dioxide: An Integrated Review of Catalysis and Life Cycle Assessment. *Chemical Reviews*. American Chemical Society January 2018, pp 434–504. https://doi.org/10.1021/acs.chemrev.7b00435.

(8) Legrand, U.; Boudreault, R.; Meunier, J. L. Decoration of N-Functionalized Graphene Nanoflakes with Copper-Based Nanoparticles for High Selectivity CO2 Electroreduction towards Formate. *Electrochim. Acta* **2019**, *318*, 142–150. https://doi.org/10.1016/j.electacta.2019.06.074.

(9) Boffito, D. C.; Fernandez Rivas, D. Process Intensification Connects Scales and Disciplines towards Sustainability. *Can. J. Chem. Eng.* **2020**, cjce.23871. https://doi.org/10.1002/cjce.23871.

(10) Artz, J.; Müller, T. E.; Thenert, K.; Kleinekorte, J.; Meys, R.; Sternberg, A.; Bardow, A.; Leitner, W. Sustainable Conversion of Carbon Dioxide: An Integrated Review of Catalysis and Life Cycle Assessment. *Chem. Rev.* **2018**, *118* (2), 434–504. https://doi.org/10.1021/acs.chemrev.7b00435.

(11) Rigamonti, M. G.; Chavalle, M.; Li, H.; Antitomaso, P.; Hadidi, L.; Stucchi, M.; Galli, F.; Khan, H.; Dollé, M.; Boffito, D. C.; Patience, G. S. LiFePO4 Spray Drying Scale-up and Carbon-Cage for Improved Cyclability. *J. Power Sources* **2020**, *462*, 228103. https://doi.org/10.1016/j.jpowsour.2020.228103.

(12) Li, H.; Cabañas-Gac, F.; Hadidi, L.; Bilodeau-Calame, M.; Abid, A.; Mameri, K.; Rigamonti, M. G.; Rousselot, S.; Dollé, M.; Patience, G. S. Ultrasound Assisted Wet Media Milling Synthesis of Nanofiber-Cage LiFePO4/C. *Ultrason. Sonochem.* **2020**, *68*, 105177. https://doi.org/10.1016/j.ultsonch.2020.105177.

(13) Whittingham, M. S. History, Evolution, and Future Status of Energy Storage. In *Proceedings of the IEEE*; Institute of Electrical and Electronics Engineers Inc., 2012; Vol.

100, pp 1518–1534. https://doi.org/10.1109/JPROC.2012.2190170.

(14) Reay, D. The Role of Process Intensification in Cutting Greenhouse Gas Emissions. *Appl. Therm. Eng.* **2008**, *28* (16), 2011–2019. https://doi.org/10.1016/j.applthermaleng.2008.01.004.

(15) Whittingham, M. S. History, Evolution, and Future Status of Energy Storage. *Proc. IEEE* **2012**, *100* (Special Centennial Issue), 1518–1534. https://doi.org/10.1109/JPROC.2012.2190170.

(16) Cano, Z. P.; Banham, D.; Ye, S.; Hintennach, A.; Lu, J.; Fowler, M.; Chen, Z. Batteries and Fuel Cells for Emerging Electric Vehicle Markets. *Nat. Energy* **2018**, *3* (4), 279–289. https://doi.org/10.1038/s41560-018-0108-1.

(17) Kane, M. Global EV Sales For 2019 Now In: Tesla Model 3 Totally Dominated.

(18) Nykvist, B.; Nilsson, M. Rapidly Falling Costs of Battery Packs for Electric Vehicles. *Nat. Clim. Chang.* **2015**, *5* (4), 329–332. https://doi.org/10.1038/nclimate2564.

(19) Edelstein, S. BMW re-ups electric-vehicle commitment—and hydrogen fuel-cell investment.

(20) Blekhman, D. Volvo's Fuel Cell Truck Alliance With Daimler Is A Return To The Hydrogen Bandwagon.

(21) Caglar, A.; Ulas, B.; Cogenli, M. S.; Yurtcan, A. B.; Kivrak, H. Synthesis and Characterization of Co, Zn, Mn, V Modified Pd Formic Acid Fuel Cell Anode Catalysts. *J. Electroanal. Chem.* **2019**, *850*, 113402. https://doi.org/10.1016/j.jelechem.2019.113402.

(22) Fernandez-Pello, A. C. Micropower Generation Using Combustion: Issues and Approaches. *Proc. Combust. Inst.* **2002**, *29* (1), 883–899. https://doi.org/10.1016/s1540-7489(02)80113-4.

(23) Ha, S.; Dunbar, Z.; Masel, R. I. Characterization of a High Performing Passive Direct Formic Acid Fuel Cell. *J. Power Sources* **2006**, *158* (1), 129–136.

https://doi.org/10.1016/j.jpowsour.2005.09.048.

(24) Zhu, Q.; Ma, J.; Kang, X.; Sun, X.; Liu, H.; Hu, J.; Liu, Z.; Han, B. Efficient Reduction of CO2into Formic Acid on a Lead or Tin Electrode Using an Ionic Liquid Catholyte Mixture. *Angew. Chemie - Int. Ed.* **2016**, *55* (31), 9012–9016. https://doi.org/10.1002/anie.201601974.

(25) Han, N.; Wang, Y.; Yang, H.; Deng, J.; Wu, J.; Li, Y.; Li, Y. Ultrathin Bismuth Nanosheets from in Situ Topotactic Transformation for Selective Electrocatalytic CO2 Reduction to Formate. *Nat. Commun.* **2018**, *9* (1), 1–8. https://doi.org/10.1038/s41467-018-03712-z.

(26) Zhu, Q.; Sun, X. F.; Kang, X. C.; MA, J.; Qian, Q. L.; Han, B. X. Cu2S on Cu Foam as Highly Efficient Electrocatalyst for Reduction of Co2 to Formic Acid. *Wuli Huaxue Xuebao/ Acta Phys. - Chim. Sin.* **2016**, *32* (1), 261–266. https://doi.org/10.3866/PKU.WHXB201512101.

(27) Marković, N. M.; Ross, P. N. Surface Science Studies of Model Fuel Cell Electrocatalysts. *Surf. Sci. Rep.* **2002**, *45* (4–6), 117–229. https://doi.org/10.1016/s0167-5729(01)00022-x.

(28) Ahmad, K. N.; Noor Azam, A. M. I.; Isahak, W. N. R. W.; Mohd Zainoodin, A.; Masdar, M. S. Improving the Electrocatalytic Activity for Formic Acid Oxidation of Bimetallic Ir-Zn Nanoparticles Decorated on Graphene Nanoplatelets. *Mater. Res. Express* **2020**, *7*, 015095. https://doi.org/10.1088/2053-1591.

(29) Yang, M.; Zhu, X.; Tang, Y.; Wu, P.; Lu, T. Highly Dispersed Ultrafine Palladium Nanoparticles on Three-Dimensional Mesoporous Carbon for Formic Acid Electro-Oxidation. *Ionics (Kiel).* **2015**, *21* (9), 2609–2614. https://doi.org/10.1007/s11581-015-1445-8.

(30) Yu, X.; Pickup, P. G. Recent Advances in Direct Formic Acid Fuel Cells (DFAFC). *J. Power Sources* **2008**, *182* (1), 124–132. https://doi.org/10.1016/j.jpowsour.2008.03.075.

(31) Rees, N. V.; Compton, R. G. Sustainable Energy: A Review of Formic Acid Electrochemical Fuel Cells. *J. Solid State Electrochem.* **2011**, *15* (10), 2095–2100. https://doi.org/10.1007/s10008-011-1398-4.

(32) Soloveichik, G. L. Liquid Fuel Cells. *Beilstein J. Nanotechnol.* **2014**, *5* (1), 1399–1418. https://doi.org/10.3762/bjnano.5.153.

(33) Fukuzumi, S. Production of Liquid Solar Fuels and Their Use in Fuel Cells. *Joule* **2017**, *1*, 689–738. https://doi.org/10.1016/j.joule.2017.07.007.

(34) Moret, S.; Dyson, P. J.; Laurenczy, G. Direct Synthesis of Formic Acid from Carbon Dioxide by Hydrogenation in Acidic Media. *Nat. Commun.* **2014**, *5* (1), 1–7. https://doi.org/10.1038/ncomms5017.

(35) Reutemann, W.; Kieczka, H. Formic Acid. In *Ullmann's Encyclopedia of Industrial Chemistry*; Wiley-VCH Verlag GmbH & Co. KGaA: Weinheim, Germany, 2011. https://doi.org/10.1002/14356007.a12_013.pub2.

(36) Bulushev, D. A.; Ross, J. R. H. Towards Sustainable Production of Formic Acid. *ChemSusChem* **2018**, *11* (5), 821–836. https://doi.org/10.1002/cssc.201702075.

(37) Rumayor, M.; Dominguez-Ramos, A.; Irabien, A. Formic Acid Manufacture: Carbon Dioxide Utilization Alternatives. *Appl. Sci.* **2018**, *8* (6), 914. https://doi.org/10.3390/app8060914.

(38) Ramdin, M.; Morrison, A. R. T.; De Groen, M.; Van Haperen, R.; De Kler, R.; Van Den Broeke, L. J. P.; Martin Trusler, J. P.; De Jong, W.; Vlugt, T. J. H. High Pressure Electrochemical Reduction of CO2 to Formic Acid/Formate: A Comparison between Bipolar Membranes and Cation Exchange Membranes. *Ind. Eng. Chem. Res.* **2019**, *58* (5), 1834–1847. https://doi.org/10.1021/acs.iecr.8b04944.

(39) Liang, S.; Altaf, N.; Huang, L.; Gao, Y.; Wang, Q. Electrolytic Cell Design for Electrochemical CO2 Reduction. *J. CO2 Util.* **2020**, *35*, 90–105. https://doi.org/10.1016/j.jcou.2019.09.007.

(40) Gong, Q.; Ding, P.; Xu, M.; Zhu, X.; Wang, M.; Deng, J.; Ma, Q.; Han, N.; Zhu, Y.; Lu, J.; Feng, Z.; Li, Y.; Zhou, W.; Li, Y. Structural Defects on Converted Bismuth Oxide Nanotubes Enable Highly Active Electrocatalysis of Carbon Dioxide Reduction. *Nat. Commun.* **2019**, *10* (1), 1–10. https://doi.org/10.1038/s41467-019-10819-4.

(41) Fan, L.; Xia, C.; Zhu, P.; Lu, Y.; Wang, H. Electrochemical CO2 Reduction to High-Concentration Pure Formic Acid Solutions in an All-Solid-State Reactor. *Nat. Commun.* **2020**, *11* (1), 1–9. https://doi.org/10.1038/s41467-020-17403-1.

(42) Ma, W.; Xie, S.; Zhang, X. G.; Sun, F.; Kang, J.; Jiang, Z.; Zhang, Q.; Wu, D. Y.; Wang, Y. Promoting Electrocatalytic CO 2 Reduction to Formate via Sulfur-Boosting Water Activation on Indium Surfaces. *Nat. Commun.* **2019**, *10* (1), 1–10. https://doi.org/10.1038/s41467-019-08805-x.

(43) Bejtka, K.; Zeng, J.; Sacco, A.; Castellino, M.; Hernández, S.; Farkhondehfal, M. A.; Savino, U.; Ansaloni, S.; Pirri, C. F.; Chiodoni, A. Chainlike Mesoporous SnO2 as a Well-Performing Catalyst for Electrochemical CO2 Reduction. *ACS Appl. Energy Mater.* **2019**, *2* (5), 3081–3091. https://doi.org/10.1021/acsaem.8b02048.

(44) Lee, W.; Kim, Y. E.; Youn, M. H.; Jeong, S. K.; Park, K. T. Catholyte-Free Electrocatalytic CO $_2$ Reduction to Formate. *Angew. Chemie Int. Ed.* **2018**, *57* (23), 6883–6887. https://doi.org/10.1002/anie.201803501.

(45) Guo, S. X.; Zhang, Y.; Zhang, X.; Easton, C. D.; MacFarlane, D. R.; Zhang, J. Phosphomolybdic Acid-Assisted Growth of Ultrathin Bismuth Nanosheets for Enhanced Electrocatalytic Reduction of CO 2 to Formate. *ChemSusChem* **2019**, *12* (5), 1091–1100. https://doi.org/10.1002/cssc.201802409.

(46) Huang, J.; Guo, X.; Yang, J.; Wang, L. Electrodeposited Bi Dendrites/2D Black Phosphorus Nanosheets Composite Used for Boosting Formic Acid Production from CO2 Electroreduction. *J. CO2 Util.* **2020**, *38*, 32–38. https://doi.org/10.1016/j.jcou.2020.01.008.

(47) Li, Z.; Zhang, T.; Yadav, R. M.; Zhang, J.; Wu, J. Boron Doping in Tin Catalysts Towards Gas-Phase CO 2 to Formic Acid/Formate Electroreduction with High Production Efficiency and Rate . *J. Electrochem. Soc.* **2020**, *167* (11), 114508. https://doi.org/10.1149/1945-7111/aba6c6.

(48) Díaz-Sainz, G.; Alvarez-Guerra, M.; Ávila-Bolívar, B.; Solla-Gullón, J.; Montiel, V.; Irabien, A. Improving Trade-Offs in the Figures of Merit of Gas-Phase Single-Pass

Continuous CO2 Electrocatalytic Reduction to Formate. *Chem. Eng. J.* **2021**, *405*, 126965. https://doi.org/10.1016/j.cej.2020.126965.

(49) Chen, Y.; Vise, A.; Klein, W. E.; Cetinbas, F. C.; Myers, D. J.; Smith, W. A.; Smith, W. A.; Smith, W. A.; Deutsch, T. G.; Neyerlin, K. C. A Robust, Scalable Platform for the Electrochemical Conversion of CO2to Formate: Identifying Pathways to Higher Energy Efficiencies. *ACS Energy Lett.* **2020**, *5* (6), 1825–1833. https://doi.org/10.1021/acsenergylett.0c00860.

(50) Xia, C.; Zhu, P.; Jiang, Q.; Pan, Y.; Liang, W.; Stavitsk, E.; Alshareef, H. N.; Wang, H. Continuous Production of Pure Liquid Fuel Solutions via Electrocatalytic CO2 Reduction Using Solid-Electrolyte Devices. *Nat. Energy* **2019**, *4* (9), 776–785. https://doi.org/10.1038/s41560-019-0451-x.

(51) Lai, Q.; Yuan, W.; Huang, W.; Yuan, G. Sn/SnOx Electrode Catalyst with Mesoporous Structure for Efficient Electroreduction of CO2 to Formate. *Appl. Surf. Sci.* **2020**, *508*, 145221. https://doi.org/10.1016/j.apsusc.2019.145221.

(52) Proietto, F.; Schiavo, B.; Galia, A.; Scialdone, O. Electrochemical Conversion of CO2 to HCOOH at Tin Cathode in a Pressurized Undivided Filter-Press Cell. *Electrochim. Acta* **2018**, *277*, 30–40. https://doi.org/10.1016/j.electacta.2018.04.159.

(53) Ramdin, M.; Morrison, A. R. T.; De Groen, M.; Van Haperen, R.; De Kler, R.; Irtem, E.; Laitinen, A. T.; Van Den Broeke, L. J. P.; Breugelmans, T.; Trusler, J. P. M.; Jong, W. De; Vlugt, T. J. H. High-Pressure Electrochemical Reduction of CO2 to Formic Acid/Formate: Effect of PH on the Downstream Separation Process and Economics. *Ind. Eng. Chem. Res.* **2019**, *58* (51), 22718–22740. https://doi.org/10.1021/acs.iecr.9b03970.

(54) Kaczur, J. J.; Yang, H.; Liu, Z.; Sajjad, S. D.; Masel, R. I. A Review of the Use of Immobilized Ionic Liquids in the Electrochemical Conversion of CO2. *C — J. Carbon Res.* **2020**, *6* (2), 33. https://doi.org/10.3390/c6020033.

(55) Han, N.; Ding, P.; He, L.; Li, Y.; Li, Y. Promises of Main Group Metal–Based Nanostructured Materials for Electrochemical CO $_2$ Reduction to Formate. *Adv. Energy*

Mater. **2020**, *10* (11), 1902338. https://doi.org/10.1002/aenm.201902338.

(56) Weekes, D. M.; Salvatore, D. A.; Reyes, A.; Huang, A.; Berlinguette, C. P. Electrolytic CO2 Reduction in a Flow Cell. *Acc. Chem. Res.* **2018**, *51* (4), 910–918. https://doi.org/10.1021/acs.accounts.8b00010.

(57) Vennekoetter, J. B.; Sengpiel, R.; Wessling, M. Beyond the Catalyst: How Electrode and Reactor Design Determine the Product Spectrum during Electrochemical CO2 Reduction. *Chem. Eng. J.* **2019**, *364*, 89–101. https://doi.org/10.1016/j.cej.2019.01.045.

(58) Jitaru, M. Electrochemical Carbon Dioxide Reduction-Fundamental and Appleid Topics (Review). *J. Univ. Chem. Technol. Metall.* **2007**, *42*, 333–344.

(59) Liu, K.; Smith, W. A.; Burdyny, T. Introductory Guide to Assembling and Operating Gas Diffusion Electrodes for Electrochemical CO 2 Reduction. *ACS Energy Lett.* **2019**, *4* (3), 639–643. https://doi.org/10.1021/acsenergylett.9b00137.

(60) Agarwal, A. S.; Zhai, Y.; Hill, D.; Sridhar, N. The Electrochemical Reduction of Carbon Dioxide to Formate/Formic Acid: Engineering and Economic Feasibility. *ChemSusChem* **2011**, *4* (9), 1301–1310. https://doi.org/10.1002/cssc.201100220.

(61) Kondratenko, E. V.; Mul, G.; Baltrusaitis, J.; Larrazábal, G. O.; Pérez-Ramírez, J. Status and Perspectives of CO2 Conversion into Fuels and Chemicals by Catalytic, Photocatalytic and Electrocatalytic Processes. *Energy Environ. Sci.* **2013**, *6* (11), 3112. https://doi.org/10.1039/c3ee41272e.

(62) MarketsandMarkets. Formic Acid Market by Types, Application & Geography - 2019 https://www.marketsandmarkets.com/Market-Reports/formic-acid-Market-69868960.html.

(63) OEC. Formic acid (HS: 291511) Product Trade, Exporters and Importers | OEC - The Observatory of Economic Complexity.

(64) IHSMarkitChem. Formic Acid. In *Chemical Economics Handbook (CEH)*; 2016.

(65) Business Wire. Research Report with COVID-19 Forecasts- Global Formic Acid Market 2020-2024 | Rising Demand for Formic Acid as a Preservative to Boost Market Growth |Technavio.

(66) Global Industry Analysts, I. Formic Acid - Global Market Trajectory & Analytics.

(67) Business Wire. Global Formic Acid Market Analysis 2020 with Forecasts to 2027: Impact of Covid-19 and a Looming Global Recession.

(68) CEIC. China | CN: Market Price: Monthly Avg: Organic Chemical Material: Formic acid 94% | Economic Indicators.

(69) Schumm, B. Fuel Cell. *Encyclopædia Britannica*; Encyclopædia Britannica, inc., 2020.

(70) Seo, E. S. M.; Yoshito, W. K.; Ussui, V.; Lazar, D. R. R.; Castanho, S. R. H. de M.; Paschoal, J. O. A. Influence of the Starting Materials on Performance of High Temperature Oxide Fuel Cells Devices. *Mater. Res.* **2004**, *7* (1), 215–220. https://doi.org/10.1590/s1516-14392004000100029.

(71) Lee, C.-G. Molten Carbonate Fuel Cells Molten Carbonate Fuel Cell (MCFC). In *Encyclopedia of Sustainability Science and Technology*; Springer New York: New York, NY, 2012; pp 6720–6740. https://doi.org/10.1007/978-1-4419-0851-3_141.

(72) Smithsonian Institution. A Basic Overview of Fuel Cell Technology.

(73) Williams, K. R. Francis Thomas Bacon, 21 December 1904 - 24 May 1992. *Biogr. Mem. Fellows R. Soc.* **1994**, *39*, 1–18. https://doi.org/10.1098/rsbm.1994.0001.

(74) Kalogirou, S. A. Industrial Process Heat, Chemistry Applications, and Solar Dryers. In *Solar Energy Engineering*; Elsevier, 2014; pp 397–429. https://doi.org/10.1016/B978-0-12-397270-5.00007-8.

(75) Abderezzak, B. Introduction to Hydrogen Technology. In *Introduction to Transfer Phenomena in PEM Fuel Cell*; Elsevier, 2018; pp 1–51. https://doi.org/10.1016/B978-1-78548-291-5.50001-9.

(76) Sudhakar, Y. N.; Selvakumar, M.; Bhat, D. K. Biopolymer Electrolytes for Fuel Cell Applications. In *Biopolymer Electrolytes*; Elsevier, 2018; pp 151–166. https://doi.org/10.1016/B978-0-12-813447-4.00005-4.

(77) Sammes, N.; Bove, R.; Stahl, K. Phosphoric Acid Fuel Cells: Fundamentals and Applications. *Curr. Opin. Solid State Mater. Sci.* **2004**, *8* (5), 372–378. https://doi.org/10.1016/j.cossms.2005.01.001.

(78) Mohapatra, A.; Tripathy, S. A Critical Review of the Use of Fuel Cells Towards Sustainable Management of Resources. *IOP Conf. Ser. Mater. Sci. Eng.* **2017**, *377*, 012135. https://doi.org/https://doi.org/10.1088/1757-899X/377/1/012135.

(79) Methanol Price|Methanol Institute|www.methanol.org https://www.methanol.org/methanol-price-supply-demand/ (accessed Nov 16, 2020).

(80) Zhao, K. *A Brief Review of China's Methanol Vehicle Pilot and Policy*; 2019.

(81) California Energy Commission. *Joint Agency Staff Report on Assembly Bill 8: 2019 Annual Assessment of Time and Cost Needed to Attain 100 Hydrogen Refueling Stations in California*; 2019.

(82) Wang, L. Q.; Bellini, M.; Filippi, J.; Folliero, M.; Lavacchi, A.; Innocenti, M.; Marchionni, A.; Miller, H. A.; Vizza, F. Energy Efficiency of Platinum-Free Alkaline Direct Formate Fuel Cells. *Appl. Energy* **2016**, *175*, 479–487. https://doi.org/10.1016/j.apenergy.2016.02.129.

(83) Wu, Q. X.; Zhao, T. S.; Chen, R.; An, L. A Sandwich Structured Membrane for Direct Methanol Fuel Cells Operating with Neat Methanol. *Appl. Energy* **2013**, *106*, 301–306. https://doi.org/10.1016/j.apenergy.2013.01.016.

(84) Wang, L.; Bambagioni, V.; Bevilacqua, M.; Bianchini, C.; Filippi, J.; Lavacchi, A.; Marchionni, A.; Vizza, F.; Fang, X.; Shen, P. K. Sodium Borohydride as an Additive to Enhance the Performance of Direct Ethanol Fuel Cells. *J. Power Sources* **2010**, *195* (24), 8036–8043. https://doi.org/10.1016/j.jpowsour.2010.06.101.

(85) Simões, M.; Baranton, S.; Coutanceau, C. Electrochemical Valorisation of Glycerol. *ChemSusChem* **2012**, *5* (11), 2106–2124. https://doi.org/10.1002/cssc.201200335.

(86) Dicks, A. L.; Rand, D. A. J. *Fuel Cell Systems Explained*; Wiley, 2018. https://doi.org/10.1002/9781118706992.

(87) Hong, P.; Zhong, Y.; Liao, S.; Zeng, J.; Lu, X.; Chen, W. A 4-Cell Miniature Direct Formic Acid Fuel Cell Stack with Independent Fuel Reservoir: Design and Performance Investigation. *J. Power Sources* **2011**, *196* (14), 5913–5917. https://doi.org/10.1016/j.jpowsour.2011.03.014.

(88) Pan, Z.; Huang, B.; An, L. Performance of a Hybrid Direct Ethylene Glycol Fuel Cell. *Int. J. Energy Res.* **2019**, *43* (7), 2583–2591. https://doi.org/10.1002/er.4176.

(89) Boffito, D. C.; Neagoe, C.; Edake, M.; Pastor-Ramirez, B.; Patience, G. S. Biofuel Synthesis in a Capillary Fluidized Bed. *Catal. Today* **2014**, *237*, 13–17. https://doi.org/10.1016/j.cattod.2014.01.018.

(90) Trevisanut, C.; Jazayeri, S. M.; Bonkane, S.; Neagoe, C.; Mohamadalizadeh, A.; Boffito, D. C.; Bianchi, C. L.; Pirola, C.; Visconti, C. G.; Lietti, L.; Abatzoglou, N.; Frost, L.; Lerou, J.; Green, W.; Patience, G. S. Micro-Syngas Technology Options for GtL. *Can. J. Chem. Eng.* **2016**, *94* (4), 613–622. https://doi.org/10.1002/cjce.22433.

(91) Yin, M.; Li, Q.; Jensen, J. O.; Huang, Y.; Cleemann, L. N.; Bjerrum, N. J.; Xing, W. Tungsten Carbide Promoted Pd and Pd-Co Electrocatalysts for Formic Acid Electrooxidation. *J. Power Sources* **2012**, *219*, 106–111. https://doi.org/10.1016/j.jpowsour.2012.07.032.

(92) Weissman, J. C.; Goebel, R. P. *Design and Analysis of Microalgal Open Pond Systems for the Purpose of Producing Fuels: A Subcontract Report*; Golden, CO, 1987. https://doi.org/10.2172/6546458.

(93) DOE Technical Targets for Hydrogen Production from Electrolysis | Department of Energy https://www.energy.gov/eere/fuelcells/doe-technical-targets-hydrogen-production-electrolysis (accessed Nov 16, 2020).

(94) Takizawa, K. Electrochemistry of Fuel Cell. In *Energy carriers and conversion systems*; Unesco-EOLSS: Tokyo, Japan, 2009.

(95) Molloy, P. Run on Less with Hydrogen Fuel Cells https://rmi.org/run-on-less-with-hydrogen-fuel-cells/.

(96) Edwards, P. P.; Kuznetsov, V. L.; David, W. I. F.; Brandon, N. P. Hydrogen and Fuel Cells: Towards a Sustainable Energy Future. *Energy Policy* **2008**, *36* (12), 4356–4362. https://doi.org/10.1016/j.enpol.2008.09.036.

(97) Maslan, N. H.; Rosli, M. I.; Masdar, M. S. Three-Dimensional CFD Modeling of a Direct Formic Acid Fuel Cell. *Int. J. Hydrogen Energy* **2019**, *44* (58), 30627–30635. https://doi.org/10.1016/j.ijhydene.2019.01.062.

(98) Sebastián, D.; Baglio, V.; Aricò, A. S.; Serov, A.; Atanassov, P. Performance Analysis of a Non-Platinum Group Metal Catalyst Based on Iron-Aminoantipyrine for Direct Methanol Fuel Cells. *Appl. Catal. B Environ.* **2016**, *182*, 297–305. https://doi.org/10.1016/j.apcatb.2015.09.043.

(99) Gasoline | 2005-2020 Data | 2021-2022 Forecast | Price | Quote | Chart | Historical https://tradingeconomics.com/commodity/gasoline (accessed Nov 16, 2020).

(100) Xia, C.; Kwok, C. Y.; Nazar, L. F. A High-Energy-Density Lithium-Oxygen Battery Based on a Reversible Four-Electron Conversion to Lithium Oxide. *Science (80-.).* **2018**, *361* (6404), 777–781. https://doi.org/10.1126/science.aas9343.

(101) Yang, J.; Yang, S.; Chung, Y.; Kwon, Y. Carbon Supported Palladium-Copper Bimetallic Catalysts for Promoting Electrochemical Oxidation of Formic Acid and Its Utilization in Direct Formic Acid Fuel Cells. *Korean J. Chem. Eng.* **2020**, *37* (1), 176–183. https://doi.org/10.1007/s11814-019-0432-6.

(102) Liu, X.; Bu, Y. F.; Cheng, T.; Gao, W.; Jiang, Q. Flower-like Carbon Supported Pd–Ni Bimetal Nanoparticles Catalyst for Formic Acid Electrooxidation. *Electrochim. Acta* **2019**, *324*, 134816. https://doi.org/10.1016/j.electacta.2019.134816.

(103) Sui, L.; An, W.; Feng, Y.; Wang, Z.; Zhou, J.; Hur, S. H. Bimetallic Pd-Based Surface Alloys Promote Electrochemical Oxidation of Formic Acid: Mechanism, Kinetics and Descriptor. *J. Power Sources* **2020**, *451*, 227830. https://doi.org/10.1016/j.jpowsour.2020.227830.

(104) Jiang, K.; Zhang, H. X.; Zou, S.; Cai, W. Bin. Electrocatalysis of Formic Acid on Palladium and Platinum Surfaces: From Fundamental Mechanisms to Fuel Cell Applications. *Phys. Chem. Chem. Phys.* **2014**, *16* (38), 20360–20376. https://doi.org/10.1039/c4cp03151b.

(105) Wang, J. Y.; Zhang, H. X.; Jiang, K.; Cai, W. Bin. From HCOOH to CO at Pd Electrodes: A Surface-Enhanced Infrared Spectroscopy Study. *J. Am. Chem. Soc.* **2011**, *133* (38), 14876–14879. https://doi.org/10.1021/ja205747j.

(106) Hu, S.; Che, F.; Khorasani, B.; Jeon, M.; Yoon, C. W.; McEwen, J. S.; Scudiero, L.; Ha, S. Improving the Electrochemical Oxidation of Formic Acid by Tuning the Electronic Properties of Pd-Based Bimetallic Nanoparticles. *Appl. Catal. B Environ.* **2019**, *254*, 685–692. https://doi.org/10.1016/j.apcatb.2019.03.072.

(107) Joo, J.; Uchida, T.; Cuesta, A.; Koper, M. T. M.; Osawa, M. The Effect of PH on the Electrocatalytic Oxidation of Formic Acid/Formate on Platinum: A Mechanistic Study by Surface-Enhanced Infrared Spectroscopy Coupled with Cyclic Voltammetry. *Electrochim. Acta* **2014**, *129*, 127–136. https://doi.org/10.1016/j.electacta.2014.02.040.

(108) Cuesta, A.; Cabello, G.; Osawa, M.; Gutiérrez, C. Mechanism of the Electrocatalytic Oxidation of Formic Acid on Metals. *ACS Catal.* **2012**, *2* (5), 728–738. https://doi.org/10.1021/cs200661z.

(109) Joo, J.; Uchida, T.; Cuesta, A.; Koper, M. T. M.; Osawa, M. Importance of Acid-Base Equilibrium in Electrocatalytic Oxidation of Formic Acid on Platinum. *J. Am. Chem. Soc.* **2013**, *135* (27), 9991–9994. https://doi.org/10.1021/ja403578s.

(110) Elnabawy, A. O.; Herron, J. A.; Scaranto, J.; Mavrikakis, M. Structure Sensitivity of Formic Acid Electrooxidation on Transition Metal Surfaces: A First-Principles Study. *J. Electrochem. Soc.* **2018**, *165* (15), J3109–J3121. https://doi.org/10.1149/2.0161815jes.

(111) Gao, W.; Keith, J. A.; Anton, J.; Jacob, T. Theoretical Elucidation of the Competitive Electro-Oxidation Mechanisms of Formic Acid on Pt(111). *J. Am. Chem. Soc.* **2010**, *132* (51), 18377–18385. https://doi.org/10.1021/ja1083317.

(112) Zhang, Y.-L.; Shen, W.-J.; Kuang, W.-T.; Guo, S.; Li, Y.-J.; Wang, Z.-H. Serrated Au/Pd Core/Shell Nanowires with Jagged Edges for Boosting Liquid Fuel Electrooxidation. *ChemSusChem* **2017**, *10* (11), 2375–2379. https://doi.org/10.1002/cssc.201700602.

(113) Fan, H.; Cheng, M.; Wang, L.; Song, Y.; Cui, Y.; Wang, R. Extraordinary Electrocatalytic Performance for Formic Acid Oxidation by the Synergistic Effect of Pt and Au on Carbon Black. *Nano Energy* **2018**, *48*, 1–9. https://doi.org/10.1016/j.nanoen.2018.03.018.

(114) Zhu, C.; Shi, Q.; Fu, S.; Song, J.; Du, D.; Su, D.; Engelhard, M. H.; Lin, Y. Core-Shell PdPb@Pd Aerogels with Multiply-Twinned Intermetallic Nanostructures: Facile Synthesis with Accelerated Gelation Kinetics and Their Enhanced Electrocatalytic Properties. *J. Mater. Chem. A* **2018**, *6* (17), 7517–7521. https://doi.org/10.1039/c7ta11233e.

(115) Xu, H.; Song, P.; Yan, B.; Wang, J.; Wang, C.; Shiraishi, Y.; Yang, P.; Du, Y. Pt Islands on 3 D Nut-like PtAg Nanocrystals for Efficient Formic Acid Oxidation Electrocatalysis. *ChemSusChem* **2018**, *11* (6), 1056–1062. https://doi.org/10.1002/cssc.201702409.

(116) Yan, X.; Hu, X.; Fu, G.; Xu, L.; Lee, J.-M.; Tang, Y. Facile Synthesis of Porous Pd_3 Pt Half-Shells with Rich "Active Sites" as Efficient Catalysts for Formic Acid Oxidation. *Small* **2018**, *14* (13), 1703940. https://doi.org/10.1002/smll.201703940.

(117) Antolini, E. Palladium in Fuel Cell Catalysis. *Energy and Environmental Science*. Royal Society of Chemistry August 2009, pp 915–931. https://doi.org/10.1039/b820837a.

(118) Weber, M. Formic Acid Oxidation in a Polymer Electrolyte Fuel Cell. *J. Electrochem. Soc.* **1996**, *143* (7), L158. https://doi.org/10.1149/1.1836961.

(119) Choi, M.; Ahn, C. Y.; Lee, H.; Kim, J. K.; Oh, S. H.; Hwang, W.; Yang, S.; Kim, J.; Kim, O. H.; Choi, I.; Sung, Y. E.; Cho, Y. H.; Rhee, C. K.; Shin, W. Bi-Modified Pt Supported on Carbon Black as Electro-Oxidation Catalyst for 300 W Formic Acid Fuel Cell Stack. *Appl. Catal. B Environ.* **2019**, *253*, 187–195. https://doi.org/10.1016/j.apcatb.2019.04.059.

(120) Jung, C.; Zhang, T.; Kim, B.-J.; Kim, J.; Kyun Rhee, C.; Lim, T.-H. Formic Acid Oxidation on Bi-Modified Pt Nanoparticles of Various Sizes. *Bull. Korean Chem. Soc.* **2010**, *31* (6), 1543. https://doi.org/10.5012/bkcs.2010.31.6.1543.

(121) Park, S.; Xie, Y.; Weaver, M. J. Electrocatalytic Pathways on Carbon-Supported Platinum Nanoparticles: Comparison of Particle-Size-Dependent Rates of Methanol, Formic Acid, and Formaldehyde Electrooxidation. *Langmuir* **2002**, *18* (15), 5792–5798. https://doi.org/10.1021/la0200459.

(122) Jiang, J.; Kucernak, A. Nanostructured Platinum as an Electrocatalyst for the Electrooxidation of Formic Acid. *J. Electroanal. Chem.* **2002**, *520* (1–2), 64–70. https://doi.org/10.1016/S0022-0728(01)00739-2.

(123) Uwitonze, N.; Chen, Y.-X. The Study of Pt and Pd Based Anode Catalysis for Formic Acid Fuel Cell. *Chem Sci J* **2017**, *8*, 3. https://doi.org/10.4172/2150-3494.1000167.

(124) Ha, S.; Larsen, R.; Zhu, Y.; Masel, R. I. Direct Formic Acid Fuel Cells with 600 MA Cm -2 at 0.4 V and 22 °C. *Fuel Cells* **2004**, *4* (4), 337–343. https://doi.org/10.1002/fuce.200400052.

(125) Ha, S.; Larsen, R.; Masel, R. I. Performance Characterization of Pd/C Nanocatalyst for Direct Formic Acid Fuel Cells. *J. Power Sources* **2005**, *144* (1), 28–34. https://doi.org/10.1016/j.jpowsour.2004.12.031.

(126) Ray, C.; Dutta, S.; Sahoo, R.; Roy, A.; Negishi, Y.; Pal, T. Fabrication of Nitrogen-Doped Mesoporous-Carbon-Coated Palladium Nanoparticles: An Intriguing Electrocatalyst for Methanol and Formic Acid Oxidation. *Chem. - An Asian J.* **2016**, *11* (10), 1588–1596. https://doi.org/10.1002/asia.201600173.

(127) Ali, H.; Zaman, S.; Majeed, I.; Kanodarwala, F. K.; Nadeem, M. A.; Stride, J. A.; Nadeem, M. A. Porous Carbon/RGO Composite: An Ideal Support Material of Highly Efficient Palladium Electrocatalysts for the Formic Acid Oxidation Reaction. *ChemElectroChem* **2017**, *4* (12), 3126–3133. https://doi.org/10.1002/celc.201700879.

(128) Zhang, Z.; Liu, S.; Tian, X.; Wang, J.; Xu, P.; Xiao, F.; Wang, S. Facile Synthesis of N-

Doped Porous Carbon Encapsulated Bimetallic PdCo as a Highly Active and Durable Electrocatalyst for Oxygen Reduction and Ethanol Oxidation. *J. Mater. Chem. A* **2017**, *5* (22), 10876–10884. https://doi.org/10.1039/c7ta00710h.

(129) Liang, X.; Liu, B.; Zhang, J.; Lu, S.; Zhuang, Z. Ternary Pd-Ni-P Hybrid Electrocatalysts Derived from Pd-Ni Core-Shell Nanoparticles with Enhanced Formic Acid Oxidation Activity. *Chem. Commun.* **2016**, *52* (74), 11143–11146. https://doi.org/10.1039/c6cc04382h.

(130) Feng, L.; Chang, J.; Jiang, K.; Xue, H.; Liu, C.; Cai, W. Bin; Xing, W.; Zhang, J. Nanostructured Palladium Catalyst Poisoning Depressed by Cobalt Phosphide in the Electro-Oxidation of Formic Acid for Fuel Cells. *Nano Energy* **2016**, *30*, 355–361. https://doi.org/10.1016/j.nanoen.2016.10.023.

(131) Xi, Z.; Li, J.; Su, D.; Muzzio, M.; Yu, C.; Li, Q.; Sun, S. Stabilizing CuPd Nanoparticles via CuPd Coupling to WO2.72 Nanorods in Electrochemical Oxidation of Formic Acid. *J. Am. Chem. Soc.* **2017**, *139* (42), 15191–15196. https://doi.org/10.1021/jacs.7b08643.

(132) Yang, G.; Chen, Y.; Zhou, Y.; Tang, Y.; Lu, T. Preparation of Carbon Supported Pd-P Catalyst with High Content of Element Phosphorus and Its Electrocatalytic Performance for Formic Acid Oxidation. *Electrochem. commun.* **2010**, *12* (3), 492–495. https://doi.org/10.1016/j.elecom.2010.01.029.

(133) Haan, J. L.; Stafford, K. M.; Masel, R. I. Effects of the Addition of Antimony, Tin, and Lead to Palladium Catalyst Formulations for the Direct Formic Acid Fuel Cell. *J. Phys. Chem. C* **2010**, *114* (26), 11665–11672. https://doi.org/10.1021/jp102990t.

(134) DandanTu; Wu, B.; Wang, B.; Deng, C.; Gao, Y. A Highly Active Carbon-Supported PdSn Catalyst for Formic Acid Electrooxidation. *Appl. Catal. B Environ.* **2011**, *103* (1–2), 163–168. https://doi.org/10.1016/j.apcatb.2011.01.023.

(135) Szumełda, T.; Drelinkiewicz, A.; Lalik, E.; Kosydar, R.; Duraczyńska, D.; Gurgul, J. Carbon-Supported Pd100-XAuX Alloy Nanoparticles for the Electrocatalytic Oxidation of Formic Acid: Influence of Metal Particles Composition on Activity Enhancement. *Appl.*

Catal. B Environ. **2018**, *221*, 393–405. https://doi.org/10.1016/j.apcatb.2017.09.039.

(136) Singh, A. K.; Singh, S.; Kumar, A. Hydrogen Energy Future with Formic Acid: A Renewable Chemical Hydrogen Storage System. *Catal. Sci. Technol.* **2016**, *6* (1), 12–40. https://doi.org/10.1039/C5CY01276G.

(137) Jiang, X.; Yan, X.; Ren, W.; Jia, Y.; Chen, J.; Sun, D.; Xu, L.; Tang, Y. Porous AgPt@Pt Nanooctahedra as an Efficient Catalyst toward Formic Acid Oxidation with Predominant Dehydrogenation Pathway. *ACS Appl. Mater. Interfaces* **2016**, *8* (45), 31076–31082. https://doi.org/10.1021/acsami.6b11895.

(138) Hu, S.; Munoz, F.; Noborikawa, J.; Haan, J.; Scudiero, L.; Ha, S. Carbon Supported Pd-Based Bimetallic and Trimetallic Catalyst for Formic Acid Electrochemical Oxidation. *Appl. Catal. B Environ.* **2016**, *180*, 758–765. https://doi.org/10.1016/j.apcatb.2015.07.023.

(139) Zhang, J.; Chen, M.; Li, H.; Li, Y.; Ye, J.; Cao, Z.; Fang, M.; Kuang, Q.; Zheng, J.; Xie, Z. Stable Palladium Hydride as a Superior Anode Electrocatalyst for Direct Formic Acid Fuel Cells. *Nano Energy* **2018**, *44*, 127–134. https://doi.org/10.1016/j.nanoen.2017.11.075.

(140) Watanabe, M.; Horiuchi, M.; Motoo, S. Electrocatalysis by Ad-Atoms. Part XXIII. Design of Platinum Ad-Electrodes for Formic Acid Fuel Cells with Ad-Atoms of the IVth and the Vth Groups. *J. Electroanal. Chem.* **1988**, *250* (1), 117–125. https://doi.org/10.1016/0022-0728(88)80197-9.

(141) Bełtowska-Brzezinska, M.; Łuczak, T.; Stelmach, J.; Holze, R. The Electrooxidation Mechanism of Formic Acid on Platinum and on Lead Ad-Atoms Modified Platinum Studied with the Kinetic Isotope Effect. *J. Power Sources* **2014**, *251*, 30–37. https://doi.org/10.1016/j.jpowsour.2013.11.027.

(142) Ferre-Vilaplana, A.; Perales-Rondón, J. V.; Feliu, J. M.; Herrero, E. Understanding the Effect of the Adatoms in the Formic Acid Oxidation Mechanism on Pt(111) Electrodes. *ACS Catal.* **2015**, *5* (2), 645–654. https://doi.org/10.1021/cs501729j.

(143) Li, H.; Zhang, Y.; Wan, Q.; Li, Y.; Yang, N. Expanded Graphite and Carbon Nanotube Supported Palladium Nanoparticles for Electrocatalytic Oxidation of Liquid Fuels. *Carbon*

N. Y. **2018**, *131*, 111–119. https://doi.org/10.1016/j.carbon.2018.01.093.

(144) Pisarek, M.; Kedzierzawski, P.; Andrzejczuk, M.; Holdyński, M.; Mikolajczuk-Zychora, A.; Borodziński, A.; Janik-Czachor, M. TiO2 Nanotubes with Pt and Pd Nanoparticles as Catalysts for Electro-Oxidation of Formic Acid. *Materials (Basel).* **2020**, *13* (5). https://doi.org/10.3390/ma13051195.

(145) Chiou, Y.-J.; Chen, M.-Y.; Chang, Y.-L.; Lin, H.-M.; Borodzinski, A. Zirconia Modified Pd Electrocatalysts for DFAFCs. *Adv. Chem. Eng. Sci.* **2020**, *10* (02), 99–112. https://doi.org/10.4236/aces.2020.102007.

(146) He, C.; Tao, J.; Ke, Y.; Qiu, Y. Graphene-Supported Small Tungsten Carbide Nanocrystals Promoting a Pd Catalyst towards Formic Acid Oxidation. *RSC Adv.* **2015**, *5* (82), 66695–66703. https://doi.org/10.1039/c5ra13028j.

(147) Pollet, B. G.; Franco, A. A.; Su, H.; Liang, H.; Pasupathi, S. Proton Exchange Membrane Fuel Cells. In *Compendium of Hydrogen Energy*; Elsevier, 2016; pp 3–56. https://doi.org/10.1016/B978-1-78242-363-8.00001-3.

(148) Barbir, F. Fuel Cell Stack Design Principles with Some Design Concepts of Micro-Mini Fuel Cells; Springer, Dordrecht, 2008; pp 27–46. https://doi.org/10.1007/978-1-4020-8295-5_3.

(149) Lanz, A.; Heffel, J.; Messer, C. Module 4: Fuel Cell Engine Technology https://www.pragma-industries.com/technology/fuel-cell-explained/.

(150) Lepiller, C. Fuel Cell Explained.

(151) Rapaport, P. A.; Rock, J. A.; Bosco, A. D.; Salvador, J. P.; Gasteiger, H. A. Fuel Cell Stack Design and Method of Operation. US6794068B2, 2004.

(152) Mathias, M. F.; Roth, J.; Fleming, J.; Lehnert, W. Diffusion Media Materials and Characterisation. In *Handbook of Fuel Cells*; John Wiley & Sons, Ltd: Chichester, UK, UK, 2010. https://doi.org/10.1002/9780470974001.f303046.

(153) Miesse, C. M.; Jung, W. S.; Jeong, K. J.; Lee, J. K.; Lee, J.; Han, J.; Yoon, S. P.; Nam, S. W.; Lim, T. H.; Hong, S. A. Direct Formic Acid Fuel Cell Portable Power System for the Operation of a Laptop Computer. *J. Power Sources* **2006**, *162* (1), 532–540. https://doi.org/10.1016/j.jpowsour.2006.07.013.

(154) Hong, P.; Liao, S. J.; Zeng, J. H.; Zhong, Y. L.; Liang, Z. X. A Miniature Passive Direct Formic Acid Fuel Cell Based Twin-Cell Stack with Highly Stable and Reproducible Long-Term Discharge Performance. *J. Power Sources* **2011**, *196* (3), 1107–1111. https://doi.org/10.1016/j.jpowsour.2010.08.111.

(155) Cai, W.; Yan, L.; Li, C.; Liang, L.; Xing, W.; Liu, C. Development of a 30 W Class Direct Formic Acid Fuel Cell Stack with High Stability and Durability. *Int. J. Hydrogen Energy* **2012**, *37* (4), 3425–3432. https://doi.org/10.1016/j.ijhydene.2011.10.120.

(156) Aslam, N. M.; Masdar, M. S.; Kamarudin, S. K.; Daud, W. R. W. Overview on Direct Formic Acid Fuel Cells (DFAFCs) as an Energy Sources. *APCBEE Procedia* **2012**, *3*, 33–39. https://doi.org/10.1016/j.apcbee.2012.06.042.

(157) Zhu, Y.; Ha, S. Y.; Masel, R. I. High Power Density Direct Formic Acid Fuel Cells. *J. Power Sources* **2004**, *130* (1–2), 8–14. https://doi.org/10.1016/j.jpowsour.2003.11.051.

(158) Dohle, H.; Divisek, J.; Mergel, J.; Oetjen, H. .; Zingler, C.; Stolten, D. Recent Developments of the Measurement of the Methanol Permeation in a Direct Methanol Fuel Cell. *J. Power Sources* **2002**, *105* (2), 274–282. https://doi.org/10.1016/S0378-7753(01)00953-3.

(159) Gogel, V.; Frey, T.; Yongsheng, Z.; Friedrich, K. .; Jörissen, L.; Garche, J. Performance and Methanol Permeation of Direct Methanol Fuel Cells: Dependence on Operating Conditions and on Electrode Structure. *J. Power Sources* **2004**, *127* (1–2), 172–180. https://doi.org/10.1016/j.jpowsour.2003.09.035.

(160) Chan, Y. H.; Zhao, T. S.; Chen, R.; Xu, C. A Small Mono-Polar Direct Methanol Fuel Cell Stack with Passive Operation. *J. Power Sources* **2008**, *178* (1), 118–124. https://doi.org/10.1016/j.jpowsour.2007.12.039.

(161) Leimin, X.; Shijun, L.; Lijun, Y.; Zhenxing, L. Investigation of a Novel Catalyst Coated

Membrane Method to Prepare Low-Platinum-Loading Membrane Electrode Assemblies for PEMFCs. *Fuel Cells* **2009**, *9* (2), 101–105. https://doi.org/10.1002/fuce.200800114.

(162) Kang, J.; Jung, D. W.; Park, S.; Lee, J. H.; Ko, J.; Kim, J. Accelerated Test Analysis of Reversal Potential Caused by Fuel Starvation during PEMFCs Operation. *Int. J. Hydrogen Energy* **2010**, *35* (8), 3727–3735. https://doi.org/10.1016/j.ijhydene.2010.01.071.

(163) Horizon. Horizon Fuel Cell Technologies. https://doi.org/https://www.horizonfuelcell.com/.

(164) FuelCellsWorks. Horizon Automotive PEM Fuel Cells to Set 300kW Benchmark - FuelCellsWorks https://fuelcellsworks.com/news/horizon-automotive-pem-fuel-cells-to-set-300kw-benchmark/.

(165) Kim, Y. S.; Lee, K.-S. Fuel Cell Membrane Characterizations. *Polym. Rev.* **2015**, *55* (2), 330–370. https://doi.org/10.1080/15583724.2015.1011275.

(166) Wang, X.; Hu, J. M.; Hsing, I. M. Electrochemical Investigation of Formic Acid Electro-Oxidation and Its Crossover through a Nafion ® Membrane. *J. Electroanal. Chem.* **2004**, *562* (1), 73–80. https://doi.org/10.1016/j.jelechem.2003.08.010.

(167) Collie, S. Formic acid joins the list of alternative fuels being put to the test https://newatlas.com/tue-bus-formic-acid/50376/.

(168) VoltaChem. Projects | CO2 Utilisation: Power-2-Formic Acid - VoltaChem https://www.voltachem.com/projects/co2-utilisation-power-2-formid-acid.

(169) FAST. Technology - Team Fast https://teamfast.nl/technology/.

(170) Maessen, J. Hydrozine: the future of fuel? https://www.intelligenttransport.com/transport-articles/69002/hydrozine-future-fuel/.

(171) Irving, M. Formic acid fuel cell carries hydrogen over infrastructure obstacles https://newatlas.com/formic-acid-fuel-cell/53887/.

(172) GRT. GRT GROUP https://grtgroup.swiss/.

(173) Laurenczy, G. Group of Catalysis for Energy and Environment https://www.epfl.ch/schools/sb/research/isic/emeritus_professors/laurenczy-gabor-hon-prof/laurenczy-gabor-hon-prof-publications/.

(174) Papageorgiou, N. The world's first formic acid-based fuel cell https://actu.epfl.ch/news/the-world-s-first-formic-acid-based-fuel-cell/.